Available online at www.sciencedirect.com
SCIENCE DIRECT
Precambrian Research 145 (2006) 131–154
Precambrian Research
www.elsevier.com/locate/precamres

Late Pan-African granitoids from the Grove Mountains, East Antarctica: Age, origin and tectonic implications

Xiaochun Liu [a,*], Bor-ming Jahn [b], Yue Zhao [a], Miao Li [a], Huimin Li [c], Xiaohan Liu [d]

[a] *Institute of Geomechanics, Chinese Academy of Geological Sciences, 11 Minzudaxue Nanlu, Beijing 100081, China*
[b] *Institute of Earth Sciences, Academia Sinica, Taipei 11529, Taiwan*
[c] *Tianjin Institute of Geology and Mineral Resources, Tianjin 300170, China*
[d] *Institute of Geology and Geophysics, Chinese Academy of Sciences, Beijing 100029, China*

Received 26 July 2005; received in revised form 20 October 2005; accepted 29 November 2005

Abstract

The Grove Mountains of East Antarctica are an inland continuation of the Pan-African Prydz Belt. The area is made up of high-grade metamorphic complex and numerous intrusive granitoid bodies including foliated charnockite, sheeted granite and charnockitic and granitic dykes. U–Pb zircon dating reveals that the charnockite, charnockitic dyke, granite and granitic dyke were emplaced in succession during the period from 550 to 500 Ma. Trace element abundances indicate that all the granitoids are of A-type affinity, characterized by enrichment in REE, Y, Ba, Sr, Ga and HFS elements (Zr, Nb, Th). Sr–Nd isotopic analyses yielded high initial $^{87}Sr/^{86}Sr$ ratios (0.7095–0.7156) and low $\varepsilon_{Nd}(T)$ values (−9.2 to −13.4). Depleted mantle-based Nd model ages range from 2.0 to 2.3 Ga. These geochemical and isotopic signatures point to their ultimate derivation from a long-term enriched subcontinental lithospheric mantle.

The charnockites of the Grove Mountains have low SiO_2 contents and high abundances of K and Ti; they are likely produced by partial melting of an alkaline basaltic protolith at elevated temperatures (980–1050 °C) at deep crust. The protolith could represent underplated magma derived from metasomatized Paleoproterozoic mantle during the late stage of the orogeny. The associated charnockitic dykes have somewhat higher SiO_2 and more distinct negative Eu, Nb, Sr, P and Ti anomalies in spidergrams, suggesting that the dykes have undergone a greater degree of fractional crystallization.

Granites were emplaced later than charnockites by 20–40 Ma. However, these two rocks have rather similar trace element and Sr–Nd isotopic characteristics, indicating that they share the same enriched basaltic source. For the granitic rocks alone, two types with different REE patterns and emplacement ages could be identified, suggesting two-stage partial melting for their derivation. Relative to charnockites, the dominant intrusive granites have slightly higher $\varepsilon_{Nd}(T)$ values, which could be compared with most metamorphic rocks from the Grove Mountains, hence a crustal contamination is implied in their petrogenesis. Granitic dykes are less silicic than granites; they were probably generated by a higher degree of melting of the same source.

Geothermobarometry of the granitoids (charnockites and granites) and associated metamorphic rocks demonstrates that the Grove Mountains underwent an earlier near-isothermal decompression of an overthickened crust, followed by a near-isobaric cooling accompanying deep emplacement (≥15 km) of granitoids during the time interval of 550–500 Ma. Implicitly, the Prydz Belt must represent a Pan-African orogen formed by collision between the Indo-Antarctic and Australo-Antarctic continental blocks.

Keywords: Charnockite; Granite; Enriched mantle; Pan-African; Grove Mountains; Prydz Belt; East Antarctica

* Corresponding author. Tel.: +86 10 68486756; fax: +86 10 68422326.
E-mail address: liuxchqw@yahoo.com.cn (X. Liu).

0301-9268/$ – see front matter © 2005 Elsevier B.V. All rights reserved.
doi:10.1016/j.precamres.2005.11.017

1. Introduction

The East Antarctic Shield, one of the Earth's oldest and largest cratonic provinces, has long been thought to have formed during the Grenvillian orogeny. However, this idea has been challenged by the revelation of widespread Pan-African high-grade metamorphism in four distinct belts within the shield: central Dronning Maud Land (Jacobs et al., 1998), Lützow-Holm Bay (Shiraishi et al., 1992), Prydz Bay (Zhao et al., 1992) and Denman Glacier (Black et al., 1992). In addition, late Pan-African granulite terranes have also been identified in other Gondwana segments, such as eastern Africa (Goscombe et al., 1998), Madagascar (Paquette et al., 1994), southern India (Choudhary et al., 1992) and Sri Lanka (Kröner and Williams, 1993). Consequently, the duration and extent of the Pan-African tectonothermal event and its implications for the formation and evolution of the Rodinia and Gondwana supercontinents have become a highly debated issue in the last decade (Fitzsimons, 2003; Harley, 2003; Meert, 2003; Yoshida et al., 2003 and references therein).

The Pan-African Prydz Belt is located in the interior of East Gondwana and it is a key element for understanding the Gondwana assembly history. However, the nature and role of this belt have always been discussed highly controversial. Some workers argue for a suture resulted from collision between the Indo-Antarctica and Australo-Antarctica continental blocks (e.g. Carson et al., 1996; Hensen and Zhou, 1997; Fitzsimons, 2000a,b; Boger et al., 2001; Zhao et al., 2003; Boger and Miller, 2004), whereas others prefer an intraplate reworking in response to the collision in the East African Orogen (e.g. Yoshida, 1995; Wilson et al., 1997; Yoshida et al., 2003). Available age data suggest that the Prydz Belt has undergone several periods of tectonothermal events since the Archaean (Hensen and Zhou, 1995; Zhao et al., 1995b; Harley et al., 1998; Boger et al., 2001). However, the polyphase deformation pattern and metamorphic recrystallization have made it difficult to identify the tectonic setting of the Prydz Belt during Pan-African time.

The Grove Mountains are situated about 200 km east of the southern Prince Charles Mountains (sPCM) (Fig. 1). They are considered as an inland continuation of the Prydz Belt based on preliminary geochronological studies (Zhao et al., 2000, 2003; Mikhalsky et al., 2001). Like Prydz Bay, the area is characterized by high-temperature granulite facies metamorphism. However, the Grove Mountains are distinguished from Prydz Bay by widespread distribution of syn- and post-orogenic granitoids. The granitoids are quite diverse in petrography and composition. They include foliated charnockites, sheeted granites and charnockitic and granitic dykes (Liu et al., 2002, 2003a,b). Since granitic rocks are often used to probe the nature and composition of the lower part of the continental crust, the granitoids of the Grove Mountains could provide information on the characteristics and tectonic process of the Prydz Belt during the Pan-African orogeny.

The purpose of this paper is to present new results of our field investigation, and petrological, geochronological and geochemical studies on the granitoids from the Grove Mountains. The new data will be used to discuss the origin and tectonic setting of the granitoids and the nature and role of the Pan-African Prydz Belt in the context of the Gondwana assembly.

2. Geological setting

The areas of Prince Charles Mountains and Prydz Bay comprise three Archaean cratonic blocks, a Grenvillian granulite terrane and a Pan-African high-grade belt (Fig. 1). The three Archaean blocks are exposed in the sPCM, Vestfold Hills and Rauer Islands. Each of them has distinct crustal histories and could not form a single unified craton (Harley, 2003). The Grenvillian terrane occurs in the northern Prince Charles Mountains (nPCM). It is characterized by regional granulite facies metamorphism accompanied by widespread charnockite magmatism at 990–940 Ma (Boger et al., 2000; Fitzsimons, 2000b). The Pan-African belt occurs in much of the area. The high-grade metamorphic rocks exposed along the Prydz Bay coastline comprise two lithological associations, mafic-felsic composite orthogneisses and migmatitic paragneisses (Fitzsimons and Harley, 1991; Dirks and Wilson, 1995). The peak metamorphic conditions were estimated at 5.5–7.0 kbar and 800–860 °C (Stüwe and Powell, 1989; Thost et al., 1994; Fitzsimons, 1996; Carson et al., 1997). Geochronological studies suggest that the high-grade metamorphism, compressional and subsequent extensional deformations, and the emplacement of syn- to post-tectonic granites all took place in a short time span of 550–490 Ma (Zhao et al., 1992, 1995b; Hensen and Zhou, 1995; Carson et al., 1996; Fitzsimons et al., 1997). However, a high-grade metamorphic event of ca. 990 Ma was also identified in a mafic granulite from Søstrene Island (Hensen and Zhou, 1995). On the other hand, Pan-African ages were also reported for the Archaean basement rocks in Rauer Islands (Harley et al., 1998; Kelsey et al., 2003) and the sPCM (Boger et al., 2001). It is obvious that the Pan-African high-grade tectonism has overprinted on the different basement provinces. Moreover, the intraplate deformation and magmatism in

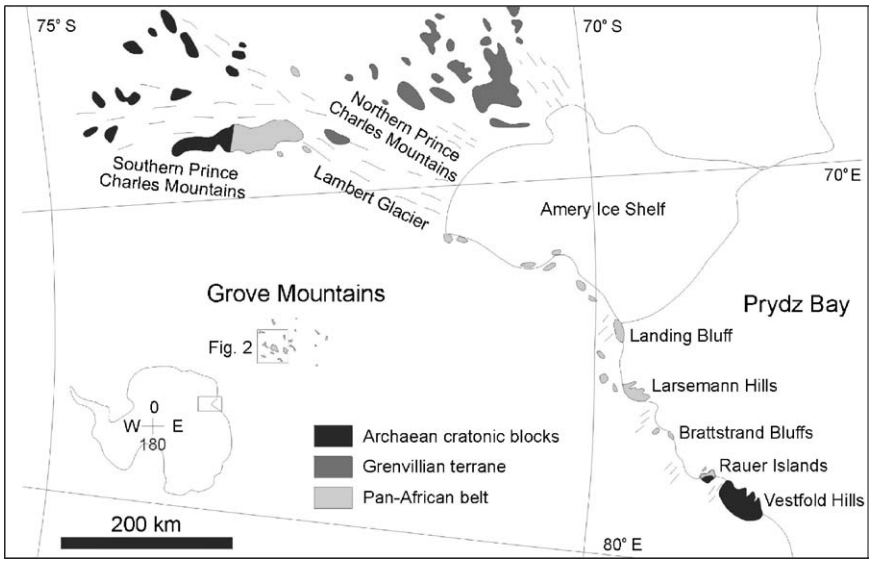

Fig. 1. Geological sketch map of the Prince Charles Mountains–Prydz Bay area and its location in East Antarctica.

response to this high-grade tectonism were recognized in the nPCM (Boger et al., 2002).

The Grove Mountains make up the southern part of the Pan-African Prydz Belt. The lithology in this area is dominated by high-grade metamorphic rocks and a variety of granitoids (Fig. 2). The metamorphic rocks comprise orthopyroxene-bearing orthogneisses and minor garnet-bearing paragneisses, mafic granulites and calc-silicate rocks (Liu et al., 2002, 2003a). Peak *P–T* conditions are estimated at 6.1–6.7 kbar and 850 °C for the granulites (Liu et al., 2003b), which are very similar to those for Prydz Bay. However, a garnet-bearing granulite appears to have preserved an earlier higher pressure record of 9.3 kbar and 800 °C (Yu et al., 2002). The granitoids include charnockites, sheeted granites and charnockitic and granitic dykes. SHRIMP U–Pb zircon dating for an orthogneiss (sample MN1-5) collected from Melwold Nunataks gave an inherited age of 910 Ma for the core, and a metamorphic age of 529 ± 14 Ma for the rim (Zhao et al., 2000). Zircons of a granite (sample E2-1) from Gale Escarpment yielded two age clusters at 534 ± 5 Ma; the rims are ca. 8 Ma younger than the internal zones (Zhao et al., 2000, 2003). An inherited age of 528 ± 5 Ma and an emplacement age of 501 ± 7 Ma was also obtained for zircon cores and rims, respectively, from a granitic dyke (sample WR3-5) in Wilson Ridge (Zhao et al., 2000). In addition, Mikhalsky et al. (2001) reported rutile and titanite U–Pb ages of 510–508 Ma for leucogneisses from Austin Nunatak, about 60 km west of the Grove Mountains. These authors also reported a young crystallization age of 504 ± 2 Ma for a so-called "charnockite" (without orthopyroxene) collected from Mount Harding. The above geochronological results suggest that the granulite facies metamorphism and emplacement of granitoids took place at ca. 530–500 Ma, which is coeval with the Pan-African event in Prydz Bay.

Structural correlation between outcrops in the Grove Mountains is difficult to establish due to the limited exposures. However, from the dominant strikes and dips of foliation, a large-scale open synform with the core at Mount Harding can be inferred (Fig. 2). This probably represents the latest regional deformation (D_3) at a shallow level during the Pan-African orogeny. A major deformation (D_2) produced a regional flat-dipping foliation in the metamorphic complex. The banding of mafic granulite in orthogneiss usually forms a series of asymmetric folds, which indicates a downslide motion of the hangingwall rocks. These subhorizontal structures should reflect crustal extension (Sandiford, 1989). The preferred orientation of metamorphic minerals with pervasive foliation suggests that the regional granulite facies metamorphism took place in an earlier stage of this deformational event (Liu et al., 2002). A still earlier compressional deformation (D_1) was recognized from a lens of fine-grained felsic gneiss surrounded and cut by mafic granulite at Mount Harding (see Fig. 3d of Liu et al., 2002). The gneissic lens exhibits a relict foliation and a steep lineation defined by the orientation of biotite, plagioclase and K-feldspar. These minerals are commonly enclosed by larger quartz crystals, suggesting late recrystallization of the quartz. Some rootless folds of

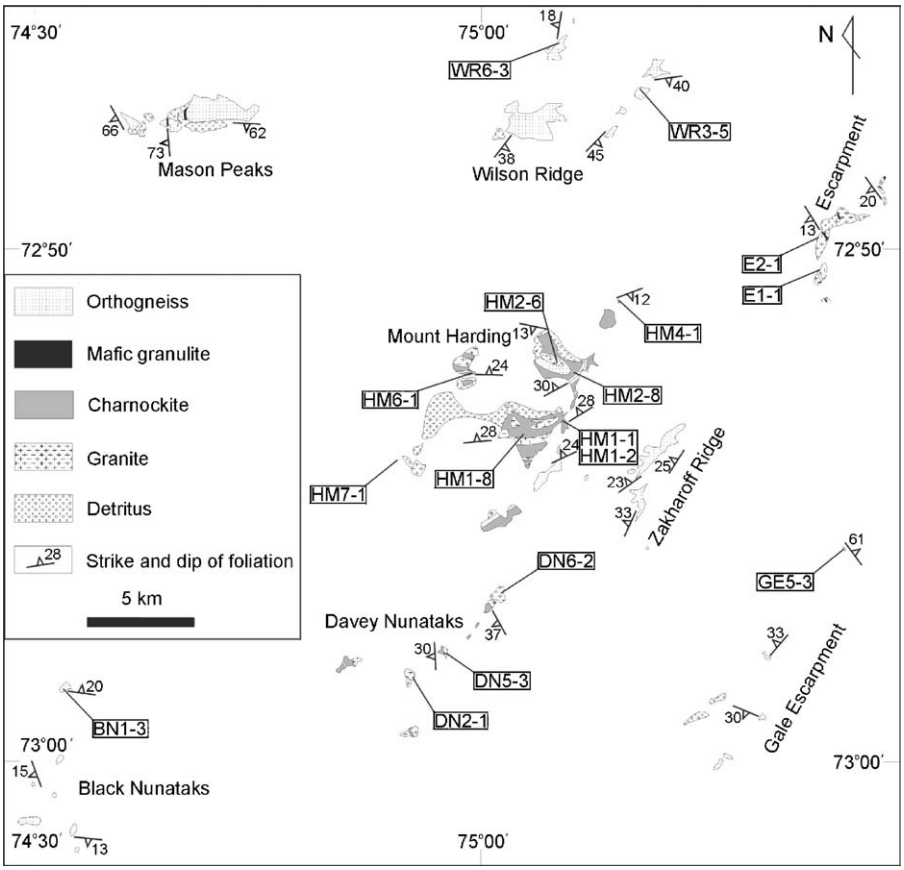

Fig. 2. Geological map of the Grove Mountains showing sampling localities.

dark bands developed within orthogneisses from Mason Peaks could be a response to this earlier event, but it is unclear if D_1 was coeval with the higher pressure granulite relics. Besides, a local deformation is recorded in some rocks, such as ductile S-C fabrics in orthogneisses, mineral orientations in charnockitic dykes, and small, open folds in granitic dykes, may indicating local shear zones.

3. Field relations of granitoids

Charnockites are mainly exposed in the areas of Mount Harding and adjacent Davey Nunataks. The rocks are typically dark brown and show weak foliation. The foliation is conformable with the D_2 gneissosity of metamorphic rocks, thus it was probably formed at the late stage of D_2. This, in turn, suggests a syn-orogenic intrusion for charnockites. The charnockites are layered as a result of the intrusion of numerous banded or sheeted granites (Fig. 3a and b). No granulite or orthogneiss xenolith has been found in charnockites.

A few charnockitic dykes are exposed in Gale Escarpment, Mount Harding and Wilson Ridge. They are about 2–10 m wide and they crosscut the foliation of country gneisses (Fig. 3c). Besides, all dykes show weak foliation, hence they were probably formed after D_2. A charnockitic dyke was found to be enclosed by a granitic dyke at Mount Harding; otherwise, no contact relationship has been observed between charnockitic dykes and charnockites or granites.

Granites occur mainly in the eastern part of the Grove Mountains, especially at Davey Nunataks and northern Gale Escarpment, where granitic bodies almost constitute the entire outcrops. Granites were emplaced as sheets of variable thickness, from a few centimeters to more than 100 m, within metamorphic rocks and charnockites (Fig. 3a and b). They in places contain xenoliths of mafic granulite, which commonly show layered texture (Fig. 3d). The contact between granites and their country rocks is nearly conformable with or slightly oblique to the foliation of country rocks. Granites do not show solid strain deformation features, but magmatic flow texture is well exhibited by strongly oriented

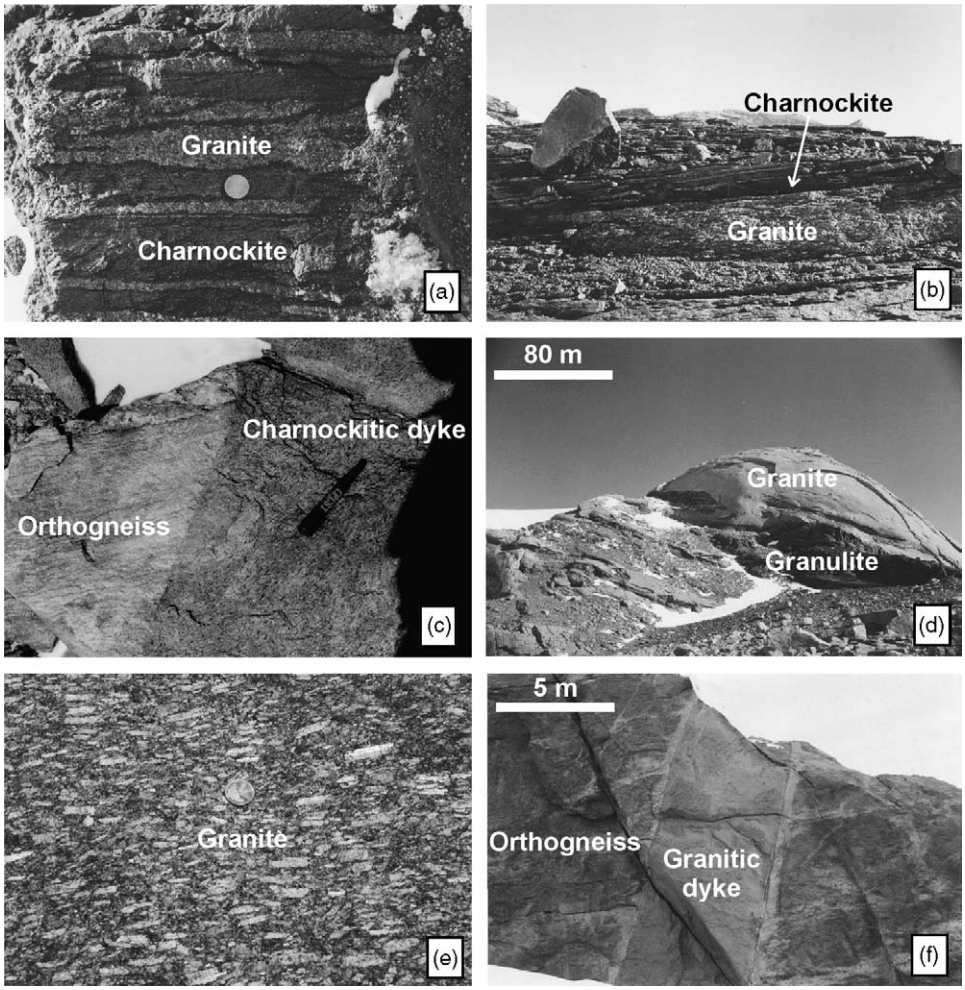

Fig. 3. Photos showing the field relations of granitoids from the Grove Mountains. (a) Layered charnockite intruded by banded granite from Mount Harding. (b) Layered charnockite intruded by sheeted granite from Mount Harding. (c) A charnockitic dyke cutting the country orthogneiss from Gale Escarpment. (d) Outcrop of granite containing mafic granulite enclaves from Gale Escarpment. (e) Orientation of K-feldspar phenocrysts in granite from Davey Nunataks. (f) A granitic dyke cutting the country orthogneiss that shows a contact thermal aureole from Black Nunataks.

K-feldspar phenocrysts (Fig. 3e). The orientation of K-feldspar phenocrysts is parallel to the gneissosity of the host rocks. No contact metamorphism has been observed in the immediate vicinity of the granitic sheets, probably implying relatively hot country rocks during magma intrusion.

Granitic dykes (0.5–20 m wide) are widespread and crosscut all metamorphic rocks and sheeted granites. Most dykes are oriented in two major directions, NE 30° and SE 120°. A contact thermal aureole was found in host orthogneisses in Black Nunataks (Fig. 3f). This suggests that metamorphic rocks have been cooled to relatively low temperatures during the emplacement of granitic dykes.

Accordingly, the major succession of intrusive activity is inferred to be from charnockites through sheeted granites to granitic dykes. The emplacement time of charnockitic dykes cannot be precisely determined, but was probably after the intrusion of charnockites and before the intrusion of granitic dykes.

4. Analytical methods

Chemical compositions of minerals were analyzed by a JEOL JXA-8800R wavelength-dispersive electron microprobe at the Institute of Mineral Deposits, Chinese Academy of Geological Sciences. The operating conditions were 20 kV accelerating voltage, 2×10^{-8} A beam current and a 2 μm beam size. The counting time at each peak was 20–30 s. Natural and synthetic minerals were used as standards. Ferric iron in orthopyroxene was determined by the scheme of Droop (1987).

Molecular formulae for amphiboles were calculated after Holland and Blundy (1994), with some corrections by Dale et al. (2000). Total iron is reported as ferrous iron in biotite.

Zircon U–Pb analyses were performed at the Tianjin Institute of Geology and Mineral Resources, China Geological Survey. Zircons were extracted from 3 to 5 kg of granitoid samples using the conventional techniques, including crushing, sieving, heavy liquid separation and hand-picking. Euhedral, homogeneous zircons without inclusions and fissures were chosen for isotopic analyses. Instrumental conditions and analytical methods were similar to those described by Xie et al. (2001) and Wu et al. (2002). Zircon dissolution and U–Pb chemical separation followed the procedures of Krogh (1973, 1982) with slight modification. Zircon grains were dissolved in HF in 0.25 ml Teflon microcapsules. A mixed ^{205}Pb–^{235}U spike was added for concentration measurement. The final isolated U and Pb were loaded on a Re filament with silica gel and phosphoric acid. U and Pb isotopic ratios were determined using a VG 354 thermal ionization mass spectrometer with Daly collector. The procedural blank was 0.05 ng for Pb and 0.002 ng for U. Ages were calculated using the following constants: $\lambda(^{238}U) = 0.155125\,Ga^{-1}$ and $\lambda(^{235}U) = 0.98485\,Ga^{-1}$. All age uncertainties are quoted at the 95% confidence level (2σ error).

Major and trace element abundances were measured by XRF (3080E) and ICP-MS (TJA PQ ExCell), respectively, at the National Research Center for Geoanalysis, Chinese Academy of Geological Sciences. FeO was separately determined by volumetry. Detailed analytical procedures for ICP-MS analysis were described by Wang et al. (2003). Analytical uncertainties range from ±1 to ±5% for major elements; ±5% for trace elements with concentrations ≥20 ppm and ±10% for concentrations ≤20 ppm. The chondritic values used in construction of REE patterns and the primitive mantle (PM) values used in spidergrams are from Sun and McDonough (1989).

Sr–Nd isotopic analyses were conducted at the Institute of Geology and Geophysics, Chinese Academy of Sciences. The analytical procedures are the same as reported by Chen et al. (2003) and Yang et al. (2004). Powder samples were weighed and spiked with ^{87}Rb, ^{84}Sr, ^{149}Sm and ^{150}Nd and then dissolved in acid ($HF + HNO_3$). Dissolution was done in Teflon vials at about 100 °C for 10 days. Rb, Sr, Sm and Nd were separated using the conventional ion exchange procedures. Mass analysis was performed using a VG 354 multicollector mass spectrometer. Sr and Nd isotopic fractionations were corrected against $^{86}Sr/^{88}Sr = 0.1194$ and $^{146}Nd/^{144}Nd = 0.7219$, respectively. During the period of data acquisition, the measured isotope ratios for NBS-607 Sr and La Jolla Nd standards were $^{87}Sr/^{86}Sr = 1.20042 \pm 2$ (2σ, $n = 12$) and $^{143}Nd/^{144}Nd = 0.511853 \pm 7$ (2σ, $n = 12$), respectively. Total procedural blanks were <500 pg for Rb and Sr, and <100 pg for Sm and Nd. Sm–Nd model ages (T_{DM}) were calculated in two ways. The one-stage model age (T^1_{DM}) is calculated assuming a linear isotopic evolution of the depleted mantle reservoir from $\varepsilon_{Nd}(T) = 0$ at 4.56 Ga to +10 at the present. The equation is:

$$T_{DM} = \frac{1}{\lambda_{Sm}} \ln\left\{1 + \frac{(^{143}Nd/^{144}Nd)_s - 0.51315}{(^{147}Sm/^{144}Nd)_s - 0.2137}\right\},$$

where s is the sample and λ_{Sm} is the decay constant of ^{147}Sm ($0.00654\,Ga^{-1}$). The two-stage model age (T^2_{DM}) is obtained assuming that the protolith of the granitic magmas has a Sm/Nd ratio (or $f_{Sm/Nd}$ value) of the average continental crust (Keto and Jacobsen, 1987):

$$T^2_{DM} = T^1_{DM} - \frac{(T^1_{DM} - t)(f_{cc} - f_s)}{f_{cc} - f_{DM}},$$

where f_{cc}, f_s and f_{DM} are the $f_{Sm/Nd}$ values of the average continental crust, sample and depleted mantle, respectively. In our calculation, $f_{cc} = -0.4$ and $f_{DM} = 0.08592$, and t is the intrusive age of granitoid.

5. Petrology and crystallization conditions

5.1. Petrography

Seventeen samples including five charnockites, two charnockitic dykes, seven granites and three granitic dykes were selected for detailed study (Fig. 2). The sample locations, mineral assemblages and field characteristics are summarized in Table 1.

Charnockites are composed of orthopyroxene (5–15%), amphibole (3–15%), biotite (<2%), plagioclase (35–45%), K-feldspar (20–30%), quartz (8–15%), ilmenite (3–5%) and trace amounts of zircon and apatite. Secondary calcite occurs in some samples. All but one sample (HM7-1) are fine- to medium-grained, and show porphyritic texture and orientation of minerals. The phenocrysts are K-feldspar and plagioclase, which, in places, contain fine-grained inclusions of amphibole, biotite and ilmenite. Amphibole in the matrix is in textural equilibrium with other minerals. Some orthopyroxene grains exhibit exsolution of lamellar magnetite. The least evolved sample, HM7-1, a floater collected on a glacier near Mount Harding, shows a typical granitic texture and unoriented structure. It contains more orthopyroxene and less amphibole than other samples.

Table 1
Field and petrographical characteristics of granitoids from the Grove Mountains

Rock type	Sample	Location	Primary minerals						Accessory and secondary minerals					Field characteristics
			Opx	Hbl	Bt	Pl	Kfs	Qtz	Mag/Ilm	Ap	Zrn	Ms	Cal	
Charnockite	HM1-1	Mt. Harding	×	×	×	×	×	×	×	×	×			Thin layer intruded by sheeted granite
	HM1-8	Mt. Harding	×	×	×	×	×	×	×	×	×		×	Thick layer intruded by sheeted granite
	HM4-1	Mt. Harding	×	×	×	×	×	×	×	×	×			Foliated without sheeted granite
	HM6-1	Mt. Harding	×	×	×	×	×	×	×	×	×			Massive, spherical weathering
	HM7-1	Mt. Harding	×	×	×	×	×	×	×	×	×		×	Floater on glacier, no foliation
Charnockitic dyke	GE5-3	Gale Escarpment	×	×	×	×	×	×	×	×	×		×	Dyke 5–10 m wide intruded in orthogneiss
	WR6-3	Wilson Ridge	×	×	×	×	×	×	×	×	×			Dyke 2 m wide intruded in orthogneiss
Granite	DN2-1	Davey Nunataks		×	×	×	×	×	×	×	×	×		Covered entire outcrop
	DN5-3	Davey Nunataks			×	×	×	×	×	×	×	×		Sheet intruded in charnockite
	DN6-2	Davey Nunataks			×	×	×	×	×	×	×	×	×	Covered entire outcrop, associated with charnockite
	HM1-2	Mt. Harding			×	×	×	×	×	×	×	×		Sheet 10 cm wide within charnockite
	HM2-6	Mt. Harding			×	×	×	×	×	×	×	×		Sheet on mountain top, overlain on orthogneiss
	E1-1	Escarpment		×	×	×	×	×	×	×	×	×		Covered entire outcrop with an orthogneiss layer
	E2-1	Escarpment		×	×	×	×	×	×	×	×		×	Covered entire outcrop with granulite inclusions
Granitic dyke	BN1-3	Black Nunataks		×	×	×	×	×	×	×	×			Dyke 5 m wide intruded in orthogneiss
	HM2-8	Mt. Harding		×	×	×	×	×	×	×	×			Dyke 20 m wide intruded in charnockite
	WR3-5	Wilson Ridge		×	×	×	×	×	×	×	×		×	Dyke 1.5 m wide intruded in orthogneiss

Abbreviations: Ap, apatite; Bt, biotite; Cal, calcite; Hbl, hornblende; Ilm, ilmenite; Kfs, K-feldspar; Mag, magnetite; Ms, muscovite; Opx, orthopyroxene; Pl, plagioclase; Qtz, quartz; Zrn, zircon.

Amphibole crystals are large and interstitial to other minerals, clearly suggesting a late crystallization.

Charnockitic dykes exhibit very similar texture and mineral assemblage to charnockites. In comparison, the dykes have more biotite (5–8%) and less orthopyroxene (3–5%) and ilmenite (2%). Orthopyroxene, amphibole, biotite and ilmenite often occur together in the matrix.

Granites are coarse-grained, with a clear orientation of K-feldspar phenocrysts. Large K-feldspar crystals can reach up to 5 cm in length. The principal phases of granites are K-feldspar (40–60%), plagioclase (15–35%), quartz (20–30%), biotite (2–5%) and magnetite/ilmenite (<2%). Amphibole (2–4%) is present only in the some samples. The main accessory minerals are zircon and apatite. Most rocks contain trace amounts of radialing secondary muscovite. Secondary calcite is occasionally present in some samples.

Granitic dykes are fine- to medium-grained with grain sizes of 0.3–1.5 mm. They consist of amphibole (5–20%), biotite (5–10%), plagioclase (20–30%), K-feldspar (30–40%), quartz (15–25%), magnetite/ilmenite (2%) and trace amounts of zircon and apatite. Secondary calcite occurs in sample WR3-5.

5.2. Mineral chemistry

The results of representative mineral analyses are presented in Table 2. Orthopyroxene is characterized by low Mg content. In charnockites it is ferrohypersthene with X_{Mg} values [=Mg/(Mg + Fe^{2+})] of 0.33–0.38, and in charnockitic dykes it is eulite with X_{Mg} values of 0.25–0.27. Amphibole in all samples is ferropargasite ($Ca_B > 1.7$; $Na_A + K_A > 0.7$; Si = 6.32–6.50 p.f.u.). It has relatively high X_{Mg} values of 0.42–0.48 in charnockites and low X_{Mg} values of 0.28–0.29 in granitic dykes. X_{Mg} values of amphibole from charnockitic dykes and granites are variable, ranging from 0.27 to 0.37 and from 0.31 to 0.39, respectively. Biotite in different type of rocks has X_{Mg} values of 0.36–0.54 and Ti contents of 0.23–0.29 p.f.u. Broadly, biotite in charnockites is richer in X_{Mg} than in other rock types. Plagioclase has homogeneous compositions and shows a negative correlation of An with SiO_2 content of whole rocks. Except for one granite sample (E2-1, An = 38), An values of plagioclase in charnockites, charnockitic dykes, granitic dykes and granites are 34–35, 32–34, 30–31 and 24–29%, respectively. Plagioclase has very low Or component, only 1–3%. K-feldspar has Or ranging from 81 to 88% except

Table 2
Electron microprobe analyses of representative minerals in granitoids from the Grove Mountains

Mineral	Sample																	
	HM6-1 (charnockite)					GE5-3 (charnockitic dyke)					E2-1 (granite)				WR3-5 (granitic dyke)			
	Opx	Hbl	Bt	Pl	Kfs	Opx	Hbl	Bt	Pl	Kfs	Hbl	Bt	Pl	Kfs	Hbl	Bt	Pl	Kfs
SiO_2	49.92	41.6	36.77	59.66	63.97	48.33	41.29	37.23	66.84	64.16	40.70	37.29	59.26	67.41	40.49	37.43	61.28	64.33
TiO_2	0.10	1.67	4.19	–	0.02	0.16	2.05	4.98	–	0.57	1.64	4.64	–	0.02	1.73	4.45	0.01	0.03
Al_2O_3	0.54	10.08	11.64	24.73	18.29	0.44	9.09	12.43	18.09	18.37	10.06	12.09	25.43	18.68	10.06	11.98	23.88	18.18
Cr_2O_3	–	0.01	–	–	–	0.01	0.06	0.12	–	–	–	–	–	–	–	–	–	0.01
FeO[a]	36.21	19.66	18.78	0.07	0.01	41.37	25.88	24.69	0.07	–	24.76	24.21	0.07	0.06	25.35	25.16	0.07	0.03
MnO	0.77	0.13	0.03	–	0.01	0.87	0.24	0.13	–	–	0.54	0.24	–	–	0.35	0.18	0.02	–
MgO	12.28	9.1	12.61	–	0.01	7.64	5.01	7.80	0.04	–	5.61	8.77	–	0.01	5.32	8.30	–	–
CaO	0.84	11.28	0.24	6.95	0.07	0.78	10.64	0.07	6.26	0.03	10.58	–	7.60	0.15	10.63	–	5.93	0.16
Na_2O	0.01	1.69	0.07	7.41	1.38	0.01	1.95	0.22	7.21	1.88	1.85	0.17	6.77	1.86	1.86	0.13	7.50	1.75
K_2O	–	1.88	9.85	0.26	15.22	–	2.04	8.71	0.34	14.39	1.85	9.89	0.28	12.80	1.93	9.84	0.26	14.98
Total	100.67	97.10	94.18	99.08	98.98	99.61	98.25	96.38	98.85	99.40	97.59	97.30	99.41	100.99	97.72	97.47	98.95	99.47
Si	1.981	6.402	2.857	2.683	2.985	1.996	6.496	2.878	2.976	2.972	6.386	2.870	2.657	3.028	6.373	2.885	2.744	2.987
Ti	0.003	0.193	0.245	–	0.001	0.005	0.242	0.290	–	0.020	0.194	0.269	–	0.001	0.205	0.258		0.001
Al	0.025	1.826	1.065	1.310	1.005	0.022	1.685	1.132	0.948	1.002	1.859	1.096	1.343	0.988	1.864	1.087	1.259	0.994
Cr	–	0.001	–	–	–	0.000	0.007	0.007	–	–	–	–	–	–	–	–	–	0.000
Fe3+	0.007	0.265	–	–	–	–	0.148	–	–	–	0.346	–	–	–	0.283	–	–	–
Fe2+	1.195	2.265	1.220	0.003	0.000	1.429	3.257	1.596	0.003	–	2.902	1.558	0.003	0.002	3.054	1.622	0.003	0.001
Mn	0.026	0.017	0.002	–	0.000	0.030	0.032	0.009	–	–	0.071	0.016	–	–	0.047	0.012	0.001	–
Mg	0.726	2.088	1.461	–	0.001	0.470	1.175	0.899	0.003	–	1.312	1.006	–	0.001	1.248	0.954	–	–
Ca	0.036	1.860	0.020	0.335	0.003	0.035	1.793	0.006	0.299	0.001	1.779	–	0.365	0.007	1.793	–	0.284	0.008
Na	0.001	0.054	0.011	0.646	0.125	0.001	0.595	0.033	0.622	0.169	0.563	0.025	0.589	0.162	0.567	0.019	0.651	0.158
K	–	0.369	0.976	0.15	0.906	–	0.410	0.859	0.019	0.850	0.370	0.971	0.016	0.734	0.388	0.968	0.015	0.887
X_{Mg}	0.38	0.48	0.54			0.25	0.27	0.36			0.31	0.39			0.29	0.37		

[a] Total iron as FeO. (–) Not detectable. Formulae of orthopyroxene, hornblende, biotite and feldspar are based on O of 6, 23, 11.5 and 8, respectively.

Table 3
Hornblende-plagioclase equilibrium temperatures and pressures for granitoids from the Grove Mountains

Rock type	Sample	T_A (°C)	T_B (°C)	P (kbar)
Charnockite	HM1-8	836	771	5.6
	HM6-1	830	751	5.7
Charnockitic dykes	GE5-3	845	796	5.0
	WR6-3	810	762	5.4
Granite	DN2-1	865	781	5.6
	E1-1	836	786	5.7
	E2-1	838	806	5.8
Granitic dykes	HM2-8	872	777	6.1
	WR3-5	843	772	5.9

T_A = edenite–tremolite thermometer of Holland and Blundy (1994); T_B = edenite–richterite thermometer of Holland and Blundy (1994); P = Al-in-hornblende barometer of Schmidt (1992).

in a granite (DN6-2, 67%) and a granitic dyke (HM2-8, 69%). An component of K-feldspar is generally less than 2%.

5.3. Crystallization conditions

Based on two reaction equilibria: (A) edenite + 4 quartz = tremolite + albite and (B) edenite + albite = richterite + anorthite, Holland and Blundy (1994) developed two thermometers for the amphibole–plagioclase paragenesis. Using thermometer A, indistinguishable crystallization temperatures of 810–870 °C (P = 6 kbar assumed) were obtained for all the granitoids from the Grove Mountains. On the other hand, thermometer B consistently yielded lower temperatures, from 750 to 810 °C (Table 3). Such discrepancy produced by the two geothermometers seems to exist for all other intrusions. John and Blundy (1994) suggest that amphibole and plagioclase coprecipitated before the appearance of quartz for $T_B < T_A$. Alternatively, this discrepancy could have been produced by the calculation of Fe^{3+} in amphibole. Because thermometer A is suitable for rocks of silica saturation, the temperatures of 810–870 °C are considered to represent near-solidus temperatures of the granitoids. In addition, the paragenesis of amphibole + biotite + plagioclase + K-feldspar + quartz + Fe–Ti oxide occurs in all types of granitoids, so the Al-in-hornblende barometer could be used to estimate crystallization/emplacement pressures. Using the calibration of Schmidt (1992), pressures of 5.0–6.1 kbar were obtained (Table 3). For some amphiboles with low X_{Mg} value, particularly those from charnockitic and granitic dykes, the upper pressure estimates may be slightly too high due to a negative X_{Mg} effect on total Al (Anderson and Bender, 1989). Note that both crystallization temperatures and pressures of all granitoids are very comparable with those of the metamorphic rocks in which they intruded (Liu et al., 2003b).

6. Geochronology

In order to determine the emplacement ages of the granitoids, we performed zircon U–Pb analyses on a charnockite (sample HM6-1) from Mount Harding, a charnockitic dyke (sample GE5-3) from Gale Escarpment, and a granite (DN6-2) from Davey Nunataks. The analytical data are given in Table 4, and illustrated in conventional concordia diagrams in Fig. 4. Note that the emplacement age of a granitic dyke (WR3-5) from Wilson Ridge has been determined at 501 ± 7 Ma by SHRIMP zircon analyses (Zhao et al., 2000).

Zircons from charnockite sample HM6-1 are transparent and pale yellow to yellowish brown. They are 150–250 μm in length, and show long and short prismatic or irregular habit, with length to width ratios of 1.5–3.0. Many grains show embayed outlines, probably implying the influence of fluid metasomatism after their formation. The analytical data on grains Nos. 1–3 are concordant, whereas the data on grains Nos. 4–7 show different degrees of discordancy produced by radiogenic Pb loss. All seven grains yield a discordia with an upper intercept age of 546 ± 6 Ma and a lower intercept age of 288 ± 34 Ma (Fig. 4a). The concordant grains Nos. 1–3 yield a weighted mean $^{206}Pb/^{238}U$ age of 547 ± 1 Ma. Because of the better precision, we take the age of 547 ± 1 Ma as the emplacement age of the charnockite. The significance of the lower intercept age of 288 ± 34 Ma is unclear. Because ages younger than 480 Ma have never been obtained for the entire Pan-

Table 4
Zircon isotopic data for granitoids from the Grove Mountains

Grain no.	Morphology	Wt (μg)	U (ppm)	Pb (ppm)	Common Pb (ng)	Isotopic ratios					Ages (Ma)		
						$^{206}Pb/^{204}Pb$	$^{208}Pb/^{206}Pb$	$^{206}Pb/^{238}U$	$^{207}Pb/^{235}U$	$^{207}Pb/^{206}Pb$	$^{206}Pb/^{238}U$	$^{207}Pb/^{235}U$	$^{207}Pb/^{206}Pb$
Charnockite (HM6-1)													
1	Irregular prism	50	1447	139	0.099	4041	0.1880	0.0885 ± 3	0.713 ± 3	0.0584 ± 1	547 ± 3	546 ± 3	544 ± 5
2	Short prism	60	1337	138	0.670	674	0.1894	0.0885 ± 3	0.713 ± 3	0.0583 ± 1	547 ± 3	546 ± 3	543 ± 4
3	Irregular prism	60	965	93	0.075	4292	0.1911	0.0884 ± 4	0.711 ± 3	0.0583 ± 8	546 ± 3	545 ± 3	543 ± 4
4	Irregular prism	60	2926	274	0.075	12611	0.2002	0.0860 ± 1	0.692 ± 1	0.0582 ± 1	532 ± 1	534 ± 1	541 ± 2
5	Long prism	20	871	70	0.12	685	0.1020	0.0742 ± 8	0.584 ± 9	0.0571 ± 6	461 ± 5	467 ± 6	494 ± 23
6	Short prism	20	1153	82	0.12	823	0.0993	0.0667 ± 6	0.516 ± 7	0.0562 ± 5	416 ± 4	423 ± 5	458 ± 21
7	Long prism	60	1141	96	1.50	201	0.1070	0.0627 ± 2	0.481 ± 3	0.0556 ± 2	392 ± 1	399 ± 2	436 ± 9
Charnockitic dyke (GE5-3)													
1	Short prism	10	372	39	0.014	1400	0.3233	0.0852 ± 19	0.681 ± 21	0.0579 ± 11	527 ± 12	527 ± 13	528 ± 43
2	Long prism	10	432	50	0.058	413	0.3256	0.0856 ± 16	0.686 ± 19	0.0582 ± 10	529 ± 10	531 ± 12	536 ± 39
3	Short prism	30	647	72	0.12	921	0.3583	0.0862 ± 8	0.694 ± 9	0.0584 ± 4	533 ± 5	535 ± 6	545 ± 17
4	Short prism	30	722	81	0.17	675	0.3608	0.0853 ± 12	0.679 ± 12	0.0577 ± 5	528 ± 7	526 ± 8	520 ± 20
5	Short prism	30	818	93	0.17	780	0.3623	0.0868 ± 8	0.697 ± 9	0.0583 ± 5	537 ± 5	537 ± 6	539 ± 18
6	Short prism	30	792	91	0.20	649	0.3624	0.0865 ± 7	0.693 ± 8	0.0582 ± 4	535 ± 5	535 ± 6	535 ± 15
7	Long prism	30	534	68	0.36	254	0.3590	0.0860 ± 11	0.689 ± 13	0.0582 ± 8	532 ± 7	532 ± 8	535 ± 29
Granite (DN6-2)													
1	Short prism	20	391	34	0.035	1167	0.1093	0.0823 ± 19	0.651 ± 21	0.0573 ± 11	510 ± 12	509 ± 13	503 ± 43
2	Long prism	20	579	55	0.18	348	0.0920	0.0810 ± 12	0.649 ± 11	0.0581 ± 8	502 ± 8	508 ± 11	535 ± 32
3	Long prism	30	387	36	0.13	474	0.0918	0.0820 ± 12	0.652 ± 14	0.0577 ± 8	508 ± 8	510 ± 9	517 ± 30
4	Long prism	30	764	67	0.19	631	0.0971	0.0807 ± 6	0.640 ± 7	0.0575 ± 4	500 ± 4	502 ± 4	510 ± 16
5	Long prism	40	1004	92	0.43	494	0.0978	0.0813 ± 4	0.646 ± 4	0.0576 ± 3	504 ± 2	506 ± 3	516 ± 11
6	Short prism	40	1436	140	0.55	544	0.1991	0.0810 ± 3	0.641 ± 3	0.0574 ± 2	502 ± 2	503 ± 2	507 ± 6
7	Short prism	40	1300	124	0.22	1241	0.2445	0.0812 ± 4	0.643 ± 4	0.0574 ± 2	503 ± 3	504 ± 3	507 ± 7

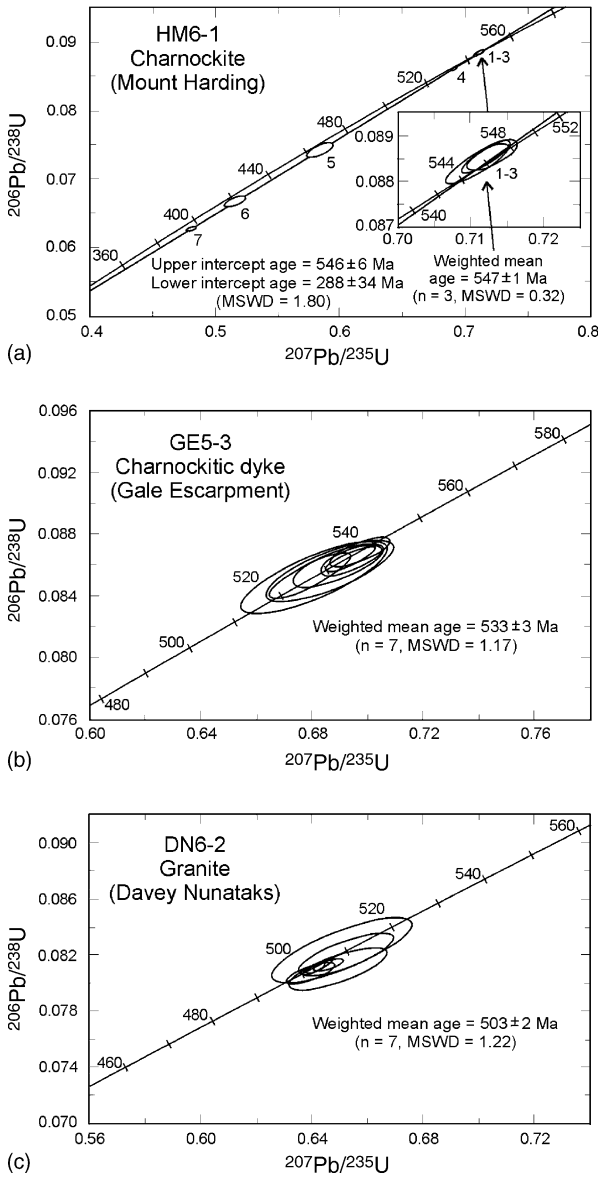

Fig. 4. U–Pb concordia diagrams for zircons from granitoid samples of the Grove Mountains. (a) Charnockite sample HM6-1 from Mount Harding. (b) Charnockitic dyke sample GE5-3 from Gale Escarpment. (c) Granite sample DN6-2 from Davey Nunataks.

African Prydz Belt, the apparent young event could be an overprint of local fluid activity.

Zircons from charnockitic dyke sample GE5-3 are transparent and pale yellow. They are euhedral and prismatic, 100–200 μm in length, and have length to width ratios of 1.5–2.0. The data of seven measured zircons are all concordant and tightly grouped. They yield a weighted mean $^{206}Pb/^{238}U$ age of 533 ± 3 Ma (Fig. 4b). We interpret the age as the time of the dyke emplacement.

Zircons from granite sample DN6-2 are also transparent and pale yellow. They are 100–200 μm in length, euhedral and prismatic, with length to width ratios of 1.5–3.0. The seven measured zircons form a concordant cluster, giving a weighted mean $^{206}Pb/^{238}U$ age of 503 ± 2 Ma (Fig. 4c). This age is taken to represent the intrusive age of the granite.

Overall, the succession of intrusive activity in the Grove Mountains as revealed by the U–Pb zircon dating coincides with the field relations of granitoids. The charnockitic dyke is confined to predate the emplacement of the granite. However, a new problem arises because the emplacement ages of intrusive charnockite and charnockitic dyke are older than the metamorphic age of an enclosing orthogneiss, which was determined at 529 Ma (Zhao et al., 2000, 2003). Since the charnockites represent high-temperature melts, they are unlikely to contain a significant amount of inherited zircons from the sources (Young et al., 1997). Therefore, the age of 547 ± 1 Ma should represent the time of zircon crystallization. Because of the small number of analyses (only four points) and large error for the age of 529 ± 14 Ma obtained for this orthogneiss, we consider that the age of metamorphism is not yet resolved. We suspect that metamorphism of the Grove Mountains could have taken place as early as ca. 550 Ma, roughly contemporaneous with the late collisional event in the East African Orogen (e.g. Kröner and Williams, 1993; Paquette et al., 1994; Shiraishi et al., 1994; Goscombe et al., 1998; Jacobs et al., 2003). Evidently, further dating of the high-grade metamorphism in the Grove Mountains is necessary. In addition, the emplacement age of 503 ± 2 Ma for granite sample DN6-2 is clearly younger than that for another granite sample E2-1 (ca. 526 Ma). Thus, the age data suggest two periods of granitic intrusion. The clear difference in geochemical characteristics between the two kinds of granite (see below) lends support to this suggestion.

7. Geochemistry

7.1. Major and trace elements

Major and trace element compositions of granitoids are listed in Table 5. Whole rock SiO_2 contents range from 55 to 59% for charnockites, 62 to 63% for charnockitic dykes, 68 to 73% for granites and 65 to 68% for granitic dykes. According to the nomenclature of Streckeisen and Le Maitre (1979), charnockite and charnockitic dyke are classified as quartz monzodiorite and quartz monzonite, whereas granite and granitic dyke as monzogranite and syenogran-

Table 5
Chemical compositions of granitoids from the Grove Mountains

	Rock type																
	Charnockite					Charnockitic dyke		Type I granite			Type II granite				Granitic dyke		
	HM1-1[a]	HM1-8[a]	HM4-1[a]	HM6-1[a]	HM7-1[a]	GE5-3[a]	WR6-3[a]	DN2-1[a]	DN5-3[a]	DN6-2[a]	HM1-2[a]	HM2-6[a]	E1-1[a]	E2-1[a]	BN1-3[a]	HM2-8[a]	WR3-5[a]
SiO_2 (wt%)	58.69	57.46	56.33	59.45	55.09	62.57	61.61	69.61	73.36	71.62	70.04	71.72	68.55	68.49	64.85	68.04	66.89
TiO_2	2.32	2.57	2.87	2.21	3.03	1.35	1.80	0.77	0.23	0.40	0.38	0.47	0.87	0.85	1.15	0.79	0.91
Al_2O_3	14.21	13.73	13.84	14.02	14.42	14.51	14.26	14.31	13.74	14.13	14.07	13.87	13.39	13.51	14.19	13.89	13.77
Fe_2O_3	2.66	2.36	2.45	2.20	3.58	1.62	2.38	1.94	0.85	1.89	1.79	1.80	2.01	1.65	2.78	2.93	2.04
FeO	6.11	6.58	7.28	5.96	7.01	4.29	5.07	1.44	0.61	0.54	0.50	0.92	2.66	2.82	3.29	1.89	3.00
MnO	0.12	0.12	0.14	0.11	0.15	0.07	0.10	0.06	0.02	0.03	0.03	0.04	0.07	0.06	0.10	0.07	0.06
MgO	2.30	2.38	2.75	2.18	2.39	1.41	1.55	0.80	0.27	0.43	0.58	0.48	0.89	0.87	1.15	0.69	0.77
CaO	5.26	5.35	5.82	4.96	5.85	3.78	4.17	2.18	1.31	1.68	1.58	1.38	2.35	2.28	2.93	2.07	2.41
Na_2O	2.95	2.98	2.77	2.98	3.10	3.12	3.13	3.02	3.09	3.16	2.19	3.22	2.81	2.85	2.89	2.68	2.89
K_2O	3.43	3.48	3.04	3.63	3.10	4.98	4.35	5.28	5.63	5.45	7.28	5.39	4.99	5.30	5.16	5.92	5.86
P_2O_5	0.88	0.95	1.14	0.82	1.21	0.45	0.65	0.27	0.05	0.12	0.25	0.13	0.25	0.25	0.38	0.21	0.21
LOI	0.55	1.83	0.90	0.92	0.86	1.25	0.51	0.67	0.52	0.58	0.65	0.74	0.62	0.67	0.74	0.63	0.71
Total	99.48	99.79	99.33	99.44	99.79	99.40	99.58	100.35	99.68	100.03	99.34	100.16	99.46	99.6	99.61	99.81	99.52
K_2O/Na_2O	1.16	1.17	1.10	1.22	1.00	1.60	1.40	1.75	1.82	1.72	3.32	1.67	1.78	1.86	1.79	2.21	2.03
A/CNK	0.78	0.75	0.75	0.79	0.76	0.83	0.82	0.98	1.01	1.00	0.98	1.02	0.94	0.93	0.91	0.95	0.89
A/NK	1.66	1.58	1.76	1.59	1.71	1.38	1.45	1.34	1.23	1.27	1.23	1.25	1.34	1.3	1.37	1.29	1.24
Rb (ppm)	84.0	142	106	124	75.4	161	151	260	282	210	309	251	271	257	157	223	193
Sr	455	497	814	548	653	554	368	343	196	246	349	164	226	209	441	192	220
Ba	1806	1531	2056	1645	2009	2734	2121	1500	827	1105	2181	854	1179	1218	2685	1663	1903
Pb	40.9	40.0	47.3	36.1	33.6	47.3	41.9	57.4	62.0	49.8	60.0	49.1	45.2	52.2	50.0	41.5	44.6
Th	25.5	22.4	13.3	14.8	7.94	12.5	11.4	14.7	14.4	77.5	19.0	86.1	81.7	120	17.6	7.53	7.76
U	2.73	2.96	1.98	2.83	1.33	0.73	1.29	3.88	2.11	2.25	3.55	5.78	6.58	8.84	1.11	1.12	0.97
Zr	757	621	426	523	679	1066	1107	420	248	354	552	341	767	654	1109	878	1116
Hf	19.8	16.5	10.7	13.7	16.3	23.7	29.6	11.1	6.84	9.46	15.7	10.3	17.2	18.1	28.6	23.2	29.5
Nb	48.5	46.7	52.2	43.7	80.9	46.3	66.8	31.4	8.20	10.4	5.82	22.9	45.7	49.5	46.7	41.4	43.7
Ta	2.65	2.65	2.87	2.53	4.06	1.99	3.19	1.83	0.41	0.46	0.31	0.77	2.40	3.09	1.91	1.57	1.71
Sc	16.0	14.9	15.6	13.4	16.7	11.2	15.1	7.28	1.27	2.83	2.45	3.95	9.36	8.99	12.6	11.2	11.5
V	122	130	147	113	121	68.5	88.5	41.1	12.2	23.4	19.6	22.0	40.2	38.6	52.2	26.2	29.3
Cr	26.3	24.9	27.8	19.5	16.0	7.85	9.66	7.32	5.93	4.69	2.30	3.48	5.38	5.25	6.22	1.83	3.09
Co	19.5	20.9	25.2	19.2	20.4	10.2	13.0	6.28	1.97	3.18	4.12	4.01	6.69	6.26	10.6	5.45	6.28
Ni	10.4	10.9	15.9	10.1	9.31	3.95	4.37	2.43	2.63	1.90	2.63	1.61	2.20	2.29	3.77	1.90	2.21
Cu	27.2	28.4	27.9	22.9	25.4	19.9	16.3	3.73	1.70	3.88	2.46	4.34	9.40	9.84	26.1	5.30	8.22
Zn	145	154	155	132	158	115	128	70.8	41.8	49.7	36.0	54.5	97.6	90.7	122	93.0	95.6
Ga	27.6	28.6	24.8	26.4	27.1	27.4	28.1	24.1	23.4	22.9	20.5	24.6	26.8	27.0	26.4	25.3	27.9
Y	53.0	50.8	42.1	44.9	51.5	43.0	58.6	28.4	10.8	12.4	22.1	31.9	73.3	82.5	60.3	60.6	51.5
K/Rb	339	203	238	243	341	257	239	169	166	215	196	178	153	171	273	220	252
Rb/Sr	0.18	0.29	0.13	0.23	0.12	0.29	0.41	0.76	1.44	0.85	0.89	1.53	1.20	1.2	0.36	1.16	0.88
Th/U	9.3	7.6	6.7	5.2	6.0	17.2	8.8	3.8	6.8	34.4	5.4	14.9	12.4	13.6	15.9	6.7	8.0
10^4Ga/Al	3.67	3.94	3.39	3.56	3.55	3.57	3.72	3.18	3.22	3.06	2.75	3.35	3.78	3.78	3.51	3.44	3.83
Y/Nb	1.09	1.09	0.81	1.03	0.63	0.93	0.88	0.90	1.32	1.19	3.80	1.39	1.60	1.67	1.29	1.46	1.18
La	198	199	183	158	172	261	195	63.2	38.1	70.5	98.5	173	323	349	294	144	161
Ce	366	370	324	284	311	456	371	137	69.3	190	155	211	533	524	437	248	285
Pr	46.6	45.2	39.7	35.7	39.9	57.9	50.4	15.7	7.01	13.8	20.1	39.1	60.6	66.0	61.7	34.1	40.5
Nd	165	160	143	127	147	208	185	55.7	22.5	45.2	70.5	129.3	207	209	227	121	150
Sm	23.4	23.0	20.7	18.8	21.8	25.9	27.9	9.17	3.92	5.90	10.1	16.9	26.6	28.0	29.3	18.4	22.7
Eu	3.66	3.72	4.01	3.33	3.99	3.79	3.67	2.18	1.20	1.27	2.61	1.51	2.03	2.05	3.80	2.40	3.21
Gd	18.9	18.6	16.8	15.8	18.4	20.4	22.6	7.66	3.31	5.25	8.36	13.5	21.9	23.3	23.4	16.2	18.16
Tb	2.13	2.08	1.84	1.83	2.12	2.10	2.60	0.99	0.42	0.52	0.98	1.65	2.60	2.77	2.65	2.01	2.25
Dy	11.0	10.6	9.11	9.36	10.8	10.0	13.3	5.31	2.10	2.51	4.49	7.94	13.9	15.1	13.6	11.3	11.9
Ho	2.09	1.96	1.66	1.76	2.03	1.81	2.48	1.00	0.32	0.49	0.84	1.41	2.69	2.98	2.52	2.24	2.21
Er	4.32	4.03	3.41	3.65	4.10	3.17	5.12	2.58	1.05	1.03	2.17	3.18	5.81	6.61	5.19	4.64	4.49
Tm	0.60	0.56	0.47	0.50	0.57	0.48	0.68	0.40	0.15	0.15	0.34	0.45	0.82	0.94	0.69	0.66	0.60
Yb	3.96	3.60	3.04	3.21	3.67	3.16	4.30	2.53	0.96	1.05	2.13	2.64	5.31	6.09	4.44	4.29	3.85
Lu	0.56	0.50	0.43	0.45	0.52	0.44	0.61	0.39	0.16	0.16	0.39	0.41	0.72	0.82	0.63	0.61	0.54
REE	846.22	842.85	751.17	663.39	737.89	1054.15	884.67	303.81	150.50	337.83	376.51	601.98	1205.98	1236.65	1105.92	609.85	706.41
$(La/Yb)_N$	36	40	43	35	34	59	33	18	28	48	33	47	44	41	48	24	30
Eu/Eu^*	0.52	0.53	0.64	0.57	0.59	0.49	0.43	0.77	0.99	0.68	0.84	0.30	0.25	0.24	0.43	0.42	0.47

[a] Sample.

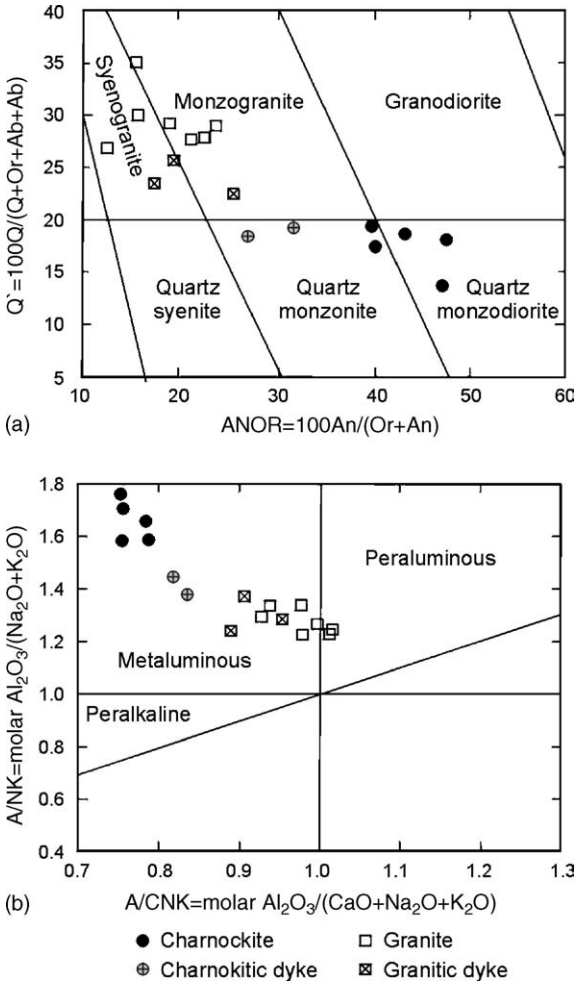

Fig. 5. (a) Classification of granitoids from the Grove Mountains using their normative compositions (after Streckeisen and Le Maitre, 1979). (b) Plot of A/NK vs. A/CNK for granitoids from the Grove Mountains (after Maniar and Piccoli, 1989).

ite, respectively (Fig. 5a). In a plot of A/NK versus A/CNK [A/CNK = molar $Al_2O_3/(CaO + Na_2O + K_2O)$], these rocks are essentially metaluminous; only two granites (samples DN5-3 and HM2-6) are peraluminous (Fig. 5b). In Harker diagrams (Fig. 6), TiO_2, FeO_t, MgO, CaO, P_2O_5, Sr, V, Cr and Zn decrease, whereas K_2O, Rb and Pb increase, with increasing SiO_2. In the SiO_2 range of 55–73%, Al_2O_3 and Na_2O are relatively constant at ca. 14% and ca. 3%, respectively. In comparison with the average compositions of Grenvillian charnockites in East Antarctica (Zhao et al., 1997), the charnockites from the Grove Mountains are more mafic and richer in TiO_2 and P_2O_5.

The chondrite-normalized rare earth element (REE) patterns of all the granitoids are strongly fractionated, with $(La/Yb)_N$ between 18 and 59 (Fig. 7). Charnockites have high total REE contents of 663–846 ppm and moderate negative Eu anomalies ($Eu/Eu^* = 0.52–0.64$). Two charnockitic dykes have even higher total REE abundances of 885–1054 ppm and larger negative Eu anomalies ($Eu/Eu^* = 0.43–0.49$). Granites may be divided into two types based on their field occurrences and both types have distinct REE patterns. Type I granites intruded into charnockites, and they have low total REE contents (151–377 ppm) and small negative to no Eu anomalies ($Eu/Eu^* = 0.68–0.99$). Type II granites, which intruded into orthogneisses, show high and variable total REE contents (602–1237 ppm) and consistent marked negative Eu anomalies ($Eu/Eu^* = 0.24–0.30$). On the other hand, granitic dykes resemble charnockitic dykes by having high total REE contents (610–1106 ppm) and large Eu anomalies ($Eu/Eu^* = 0.42–0.47$).

In the primitive mantle normalized spidergrams (Fig. 8), all the granitoids exhibit high abundances of Rb, Th, K, Zr and La (REE), and relative depletion in Nb, Sr, P and Ti. Granites differ slightly from charnockites in weakly depleted Ba and larger negative Nb, Sr, P and Ti anomalies. Generally, the granitoids from the Grove Mountains have high Ba and Sr contents and low Rb/Sr ratios. In addition, some samples have much higher Th contents and Th/U ratios (up to >10) than the estimated crustal average (3.8, Taylor and McLennant, 1985), which are similar to the Cambrian granitoids from eastern Amery Ice Shelf and Prydz Bay (Sheraton and Black, 1988; Sheraton et al., 1996).

Trace element geochemistry also indicates that all granitoids from the Grove Mountains have an A-type affinity, just as the Cambrian granites from eastern Amery Ice Shelf, nPCM and sPCM (Manton et al., 1992; Sheraton et al., 1996). These rocks are characterized by marked enrichment in Ga, Zr, Nb and Y. $10^4 Ga/Al$ ratios of the rocks range from 2.75 to 3.94, with average values of 3.42 for charnockites and 3.30 for granites (Fig. 9). In Nb versus Y and Rb versus (Y + Nb) diagrams of Pearce et al. (1984), most samples fall in the field of within-plate granites (WPG); only three granites (samples DN5-3, DN6-2 and HM1-2) fall in the field of syncollisional granites (Fig. 10). Y/Nb ratios of different rocks are distinctive, <1.10 for charnockites and charnockitic dykes and >1.18 for most granites (except sample DN2-1) and granitic dykes.

7.2. Sr–Nd isotope characteristics

Rb–Sr and Sm–Nd isotopic data of the granitoids are presented in Table 6. Overall, all the granitoids display uniform and evolved isotopic signatures. They

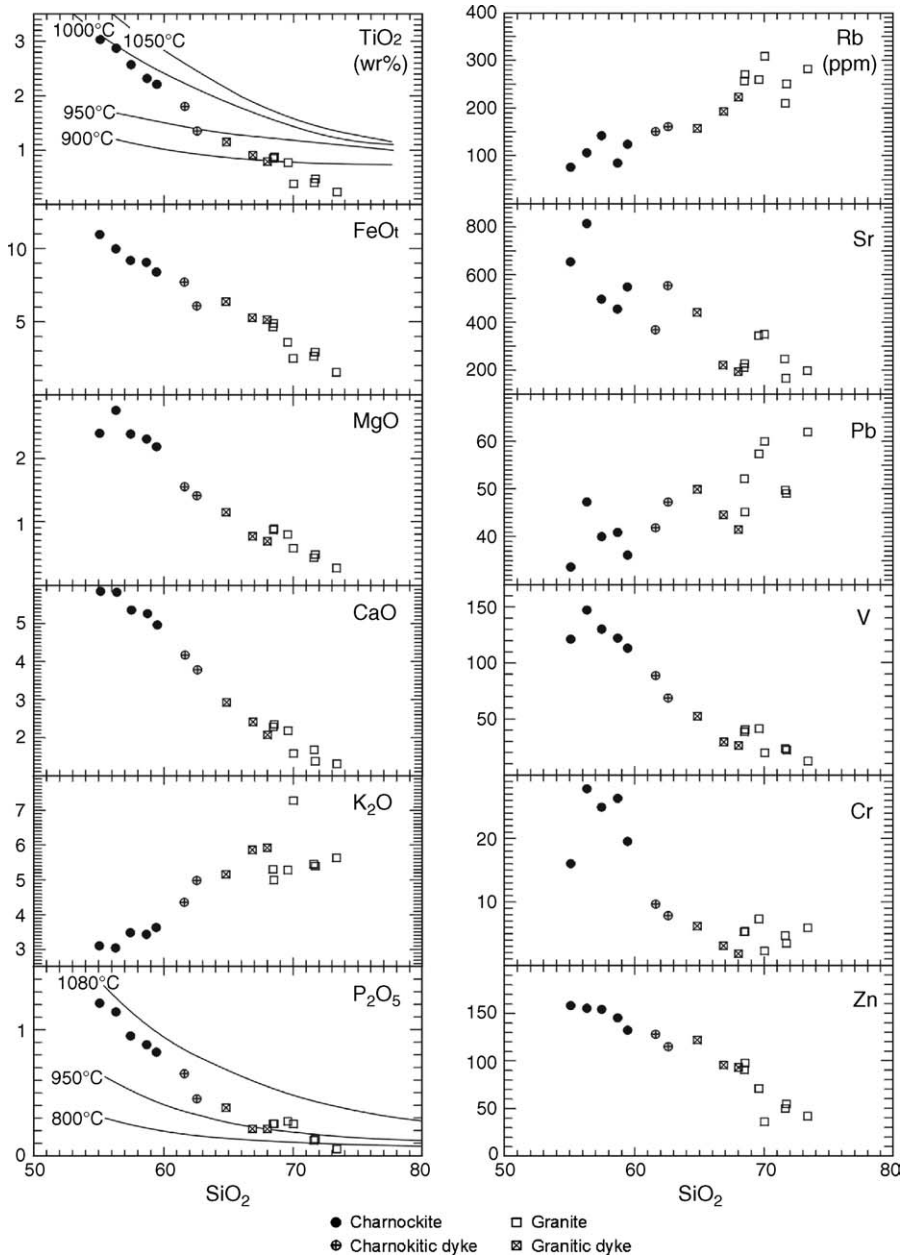

Fig. 6. Harker diagrams for major and trace elements of granitoids from the Grove Mountains. The isotherms in TiO_2–SiO_2 and P_2O_5–SiO_2 plots show Fe–Ti oxide and apatite saturation temperatures at 7.5 kbar (after Green and Watson, 1982; Green and Pearson, 1986).

have small ranges of initial $^{87}Sr/^{86}Sr$ ratios (I_{Sr}) of 0.7095–0.7156, and initial ε_{Nd} values [$\varepsilon_{Nd}(T)$] of −9.2 to −13.4 (Fig. 11a and b). Because many samples have $^{147}Sm/^{144}Nd$ ratios (<0.10) lower than the average crustal ratio of 0.12, we consider that the two-stage Nd model ages are more realistic for inferring the age of the source. As shown in Table 6, all T^2_{DM} values range from 2.0 to 2.3 Ga, but granites tend to be slightly younger than charnockites. These ages are comparable with the Pan-African orthogneisses from Prydz Bay (Hensen and Zhou, 1995) and the Grenvillian charnockites from nPCM and Mawson Coast (Zhao et al., 1997; Young et al., 1997). Note that isotopic compositions of granitoids from the Grove Mountains are very similar to those of the Pan-African syenitic rocks from David Island, west of Denman Glacier (Sheraton et al., 1992; see Fig. 11a). This locality could be linked to the Prydz Belt (Fitzsimons, 2000a,b).

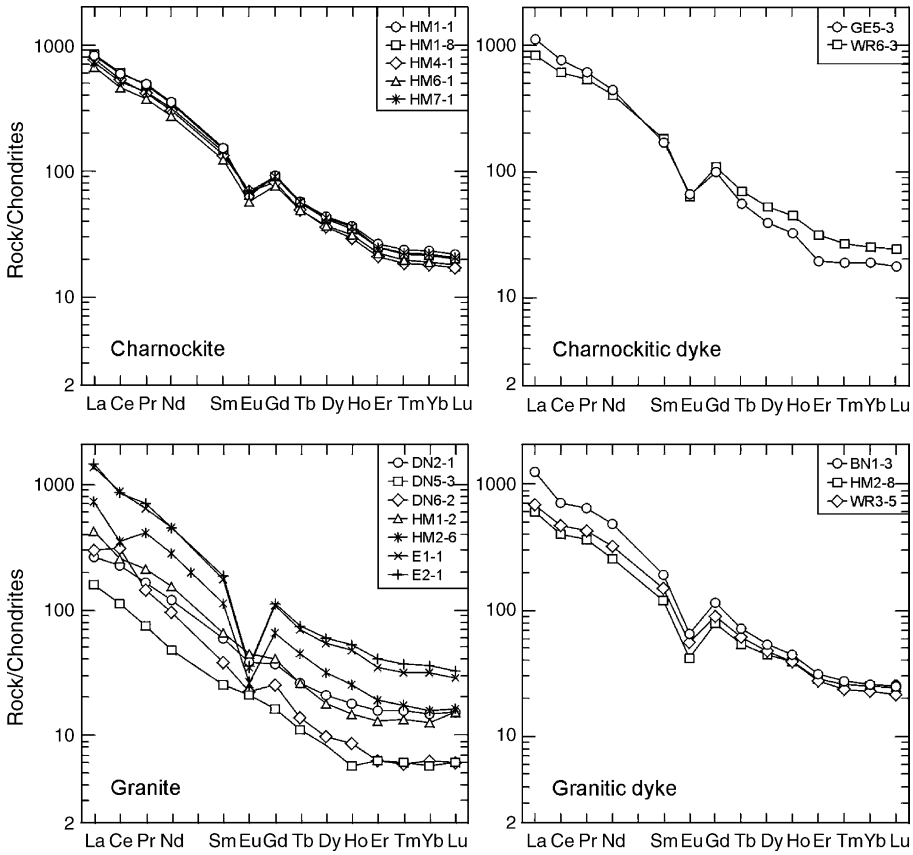

Fig. 7. Chondrite-normalized REE patterns for granitoids from the Grove Mountains. Chondrite values used for normalization are from Sun and McDonough (1989).

8. Origin of granitoids

8.1. Charnockite and charnockitic dykes

There are two major models for the origin of charnockite, metamorphic and igneous. In the Grove Mountains, the single age and distinct high TiO_2, P_2O_5 and K_2O contents of charnockites as well as the occurrence of charnockitic dykes strongly suggest their igneous origin, although no intrusive contact between charnockites and their country rocks could be observed due to the late deformation and granite emplacement. Geochemically, charnockites from the Grove Mountains are similar to those from nPCM (Zhao et al., 1997) and adjacent Mawson Coast (Young et al., 1997) as well as most charnockites elsewhere (e.g. Kilpatrick and Ellis, 1992; Sheraton et al., 1992). However, a distinctive mineralogical feature is that they contain more amphiboles (3–15%), which, except those in sample HM7-1, are in equilibrium with other minerals. Experimental studies suggest that hot, relatively dry granitic magmas may crystallize pyroxenes during early stages of differentiation, whilst at later stages, at lower temperatures or high water and oxygen fugacities, amphibole or biotite can be produced (Green and Lambert, 1965; Naney, 1983). If this is the case, the charnockites from the Grove Mountains could have formed at the later stages of magmatic evolution. Moreover, these charnockites could have been subjected to recrystallization in the presence of fluid during deformation. In fact, an undeformed sample HM7-1 that contains a lesser amount of amphibole may lend support to our interpretation.

High concentrations of TiO_2, P_2O_5 and Zr reflect high-temperature partial melting and fractionation for the origin of the charnockite magma. TiO_2 and P_2O_5 versus SiO_2 contents of charnockites from the Grove Mountains yield saturation temperatures of ilmenite and apatite of about 980–1050 °C at 7.5 kbar (see Fig. 6; Green and Watson, 1982; Green and Pearson, 1986). The generation of such high-temperature magma requires water-absent and CO_2-flushed conditions (Kilpatrick and Ellis, 1992; Zhao et al., 1997), which are a diagnostic feature of granulite facies metamorphism in the lower crust. Despite small variation of SiO_2 contents, the correlation between

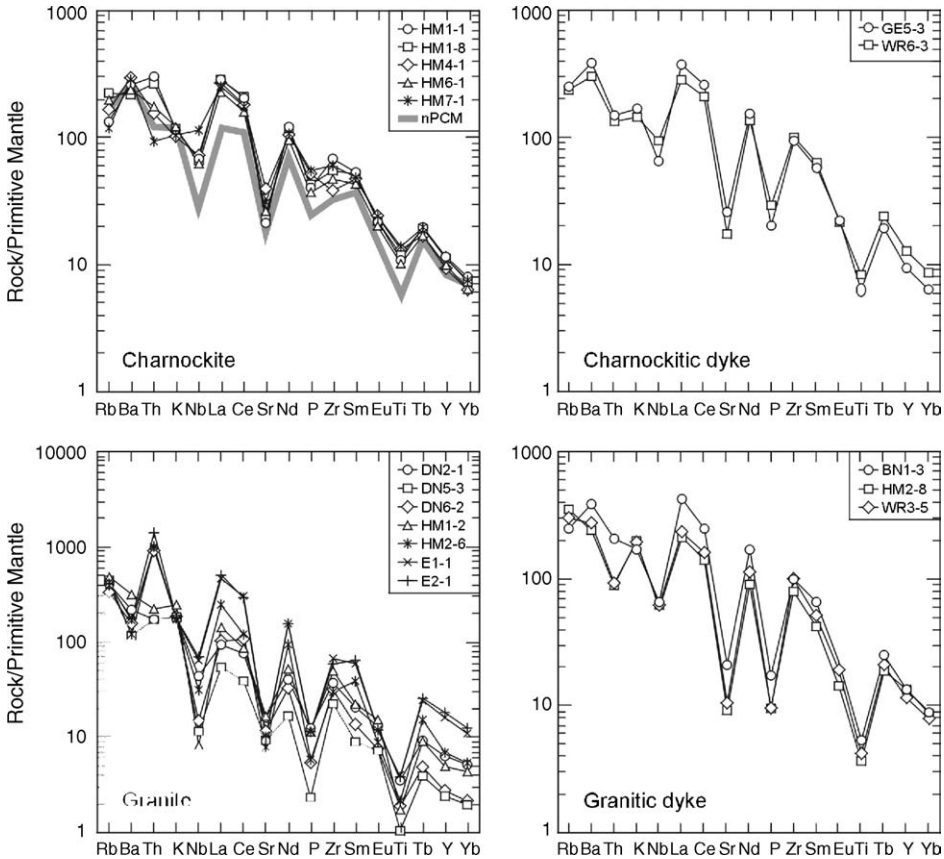

Fig. 8. Primitive mantle (PM) normalized spidergrams for granitoids from the Grove Mountains. Charnockites show similar patterns to the average charnockite from northern Prince Charles Mountains (nPCM; after Zhao et al., 1997). The PM values used for normalization are from Sun and McDonough (1989).

certain elements and SiO_2 of charnockites probably indicates involvement of fractional crystallization. Negative Eu, Sr, Nb, Ti and P anomalies and their decrease with increasing SiO_2 suggest that fractionation of feldspar, ilmenite and apatite played an important role in the genesis of the charnockite magma.

The compositions of charnockites from the Grove Mountains indicate that their major sources must be basaltic, rather than intermediate as inferred by Zhao et al. (1997) and Young et al. (1997) for the nPCM and Mawson charnockites. With respect to the geochemical features of the Grove Mountains charnockites, a high-K and high-Ti basaltic source rock is required. The high I_{Sr} values of 0.7119–0.7134, low $\varepsilon_{Nd}(T)$ values of −10.9 to −12.2, and strong enrichment in REE, Ba and certain HFS elements, such as Zr, Hf, Th and Y, cannot be interpreted by crustal contamination in the generation of the charnockites. Such distinct geochemical features should have been inherited from a long-term enriched lithospheric mantle produced by previously subduction-related processes (McCulloch and Gamble, 1991). In fact, similar enriched mantle sources have been identified for Cambrian igneous rocks from many places in East Antarctica, such as Priestley Peak (Nelson and McCulloch, 1989), Bunger Hills (Sheraton et al., 1990), David Island (Sheraton et al., 1992) and the Yamato Mountains (Zhao et al., 1995a). The isotopic distinction (Fig. 11a) of different places is probably due to differences in the time of mantle enrichment, as also suggested by Zhao et al. (1995a). Nd model ages of 2.2–2.3 Ga for the charnockites suggest that mantle enrichment of the Grove Mountains rocks probably occurred during the Paleoproterozoic, contemporaneous with continental crust formation in the area. Accordingly, we infer that the underplating of enriched mantle-derived basalt occurred during late Pan-African orogeny in the Grove Mountains. These basaltic materials were later partially melted to produce charnockite magma.

The close similarity in geochemical and isotopic characteristics between charnockitic dykes and charnockites suggests that they were derived by partial melting of the same source rocks, although the dykes postdate the

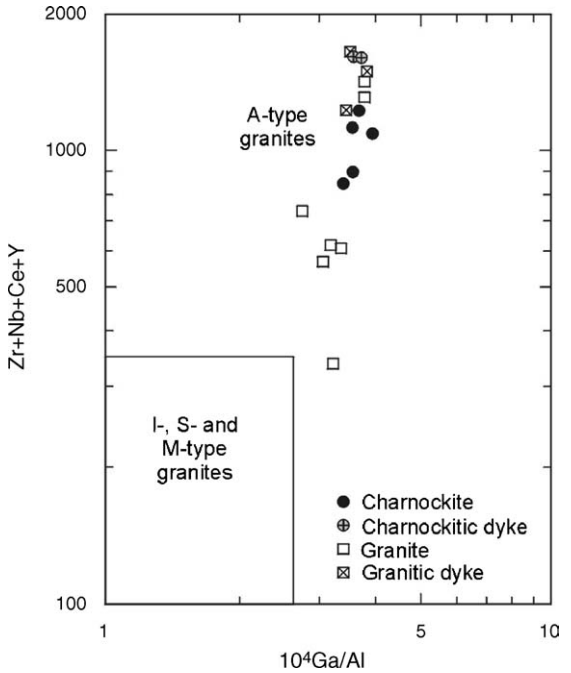

Fig. 9. Plot of 10^4Ga/Al vs. Zr + Nb + Ce + Y for granitoids from the Grove Mountains (after Whalen et al., 1987).

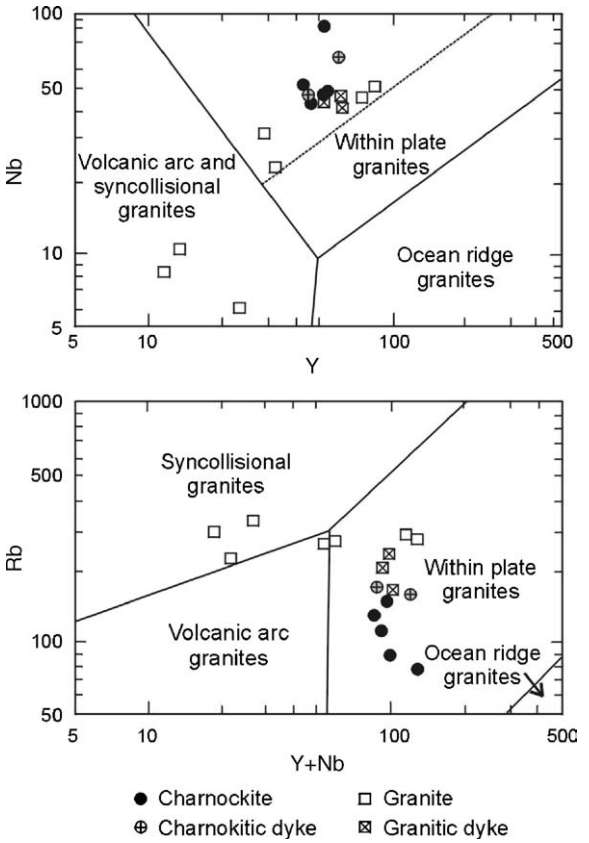

Fig. 10. Plots of Nb vs. Y and Rb vs. Y + Nb for granitoids from the Grove Mountains (after Pearce et al., 1984).

emplacement of charnockites by about 15 Ma. The relatively high SiO_2 and more distinct negative Eu, Nb, Sr, P and Ti anomalies imply that charnockitic dykes experienced a stronger fractional crystallization than charnockites. An acceptable interpretation is that the charnockitic dykes are the products of the latest fractionation of charnockite magma from the same chamber.

8.2. Granite and granitic dykes

A striking feature of the granitoids from the Grove Mountains is the close association of granites and charnockites. The granites intruded into charnockites and postdate the charnockites by about 20–40 Ma. The initial $^{87}Sr/^{86}Sr$ ratios, initial $\varepsilon_{Nd}(T)$ values, and Nd model ages are all comparable between the two magmatic suits. Likewise, granites and charnockites are strongly enriched in REE, Ba and some HFS elements such as Zr, Hf, Th and Y. All the above characteristics suggest a close genetic link between charnockites and granites. They probably share the same basaltic source derived from an enriched subcontinental lithospheric mantle. With respect to their petrogenesis, the granites could have been produced by fractional crystallization from the charnockitic magma or by partial melting of the enriched basaltic source. Many granite samples have smaller negative Eu anomalies (even almost no Eu anomaly in one sample) as compared with charnockites. This may argue against the model of fractional crystallization. The high Ba and Sr contents and low Rb/Sr ratios of granites are also in conflict with a fractional crystallization model (Halliday et al., 1991). We therefore prefer a partial melting model of basaltic rocks for granites from the Grove Mountains. The heat responsible for partial melting of such rocks could have come from the basaltic underplating during crustal extension.

However, relative to charnockites, granites tend to have slightly higher initial $\varepsilon_{Nd}(T)$ values and younger ages (see Fig. 11). Nd isotopic analyses reveal that the initial $\varepsilon_{Nd}(T)$ values of most metamorphic rocks from the Grove Mountains are higher than those of the Pan-African granitoids. They are −0.8 to −3.7 for orthogneisses, except for two samples with $\varepsilon_{Nd}(T)$ of −10.4 to −10.7 (t = 910 Ma), +0.8 to −1.9 for mafic granulites (t = 910 Ma), and −7.4 to −8.8 for paragneisses except for one sample with $\varepsilon_{Nd}(T)$ of −24.5 (t = 550 Ma) (our unpublished data; see Fig. 11b). This suggests that crustal contamination played a role in the

Table 6
Sr–Nd isotopic analyses for granitoids from the Grove Mountains

Sample	Rb (ppm)	Sr (ppm)	$^{87}Rb/^{86}Sr$	$^{87}Sr/^{86}Sr$	I_{Sr}	Sm (ppm)	Nd (ppm)	$^{147}Sm/^{144}Nd$	$^{143}Nd/^{144}Nd$	$f_{Sm/Nd}$	$\varepsilon_{Nd}(0)$	$\varepsilon_{Nd}(T)$	T^1_{DM}(Ga)	T^2_{DM}(Ga)
Charnockite (t = 547 Ma)														
HM1-1	129.3	497.1	0.747	0.718891 ± 11	0.7131	25.86	164.6	0.0951	0.511653 ± 11	−0.52	−19.2	−12.1	1.92	2.25
HM1-8	136.8	454.6	0.866	0.720111 ± 16	0.7134	24.98	150.11	0.1007	0.511673 ± 08	−0.49	−18.2	−12.1	1.99	2.25
HM4-1	103.9	764.8	0.391	0.715353 ± 10	0.7123	22.59	137.66	0.0993	0.511662 ± 11	−0.50	−19.0	−12.2	1.98	2.26
HM6-1	132.8	533.2	0.720	0.718190 ± 14	0.7126	20.20	120.10	0.1018	0.511708 ± 11	−0.48	−18.1	−11.5	1.96	2.20
HM7-1	79.0	622.6	0.367	0.714786 ± 16	0.7119	23.38	139.67	0.1014	0.511737 ± 09	−0.48	−17.6	−10.9	1.91	2.15
Charnockitic dykes (t = 533 Ma)														
GE5-3	175.3	551.3	0.914	0.717742 ± 14	0.7108	27.67	184.87	0.0906	0.511702 ± 11	−0.54	−18.3	−11.0	1.79	2.15
WR6-3	166.1	401.8	1.190	0.724072 ± 14	0.7150	31.44	183.41	0.1038	0.511629 ± 06	−0.47	−19.7	−13.4	2.10	2.34
Type I granite (t = 503 Ma)														
DN2-1	272.2	347.9	2.253	0.729231 ± 17	0.7131	10.28	55.90	0.1113	0.511747 ± 09	−0.43	−17.4	−11.9	2.08	2.19
DN5-3	284.3	209.2	3.919	0.743295 ± 14	0.7152	4.10	22.41	0.1109	0.511817 ± 11	−0.44	−16.0	−10.5	1.97	2.08
DN6-2	206.9	240.3	2.468	0.731063 ± 13	0.7134	6.88	45.19	0.0922	0.511789 ± 11	−0.53	−16.6	−9.9	1.70	2.03
HM1-2	337.0	396.1	2.450	0.732635 ± 13	0.7151	10.18	67.16	0.0918	0.511715 ± 13	−0.53	−18.0	−11.3	1.79	2.14
Type II granite (t = 526 Ma)														
HM2-6	264.6	177.8	4.281	0.747687 ± 14	0.7156	18.82	126.6	0.0900	0.511801 ± 12	−0.54	−16.3	−9.2	1.66	1.99
E1-1	282.2	225.8	3.598	0.739052 ± 11	0.7121	29.41	192.05	0.0927	0.511755 ± 12	−0.53	−17.2	−10.2	1.75	2.08
E2-1	293.9	241.2	3.516	0.739595 ± 14	0.7132	30.07	195.51	0.0931	0.511749 ± 18	−0.53	−17.3	−10.4	1.77	2.09
Granitic dykes (t = 501 Ma)														
BN1-3	214.8	458.8	1.345	0.719130 ± 15	0.7095	32.53	213.44	0.0923	0.511650 ± 16	−0.53	−19.3	−12.6	1.88	2.25
HM2-8	227.2	191.3	3.428	0.738437 ± 11	0.7140	21.45	123.25	0.1053	0.511815 ± 08	−0.46	−16.1	−10.2	1.87	2.05
WR3-5	226.3	252.2	2.610	0.731804 ± 10	0.7132	29.43	169.72	0.1050	0.511765 ± 10	−0.47	−17.0	−11.2	1.94	2.13

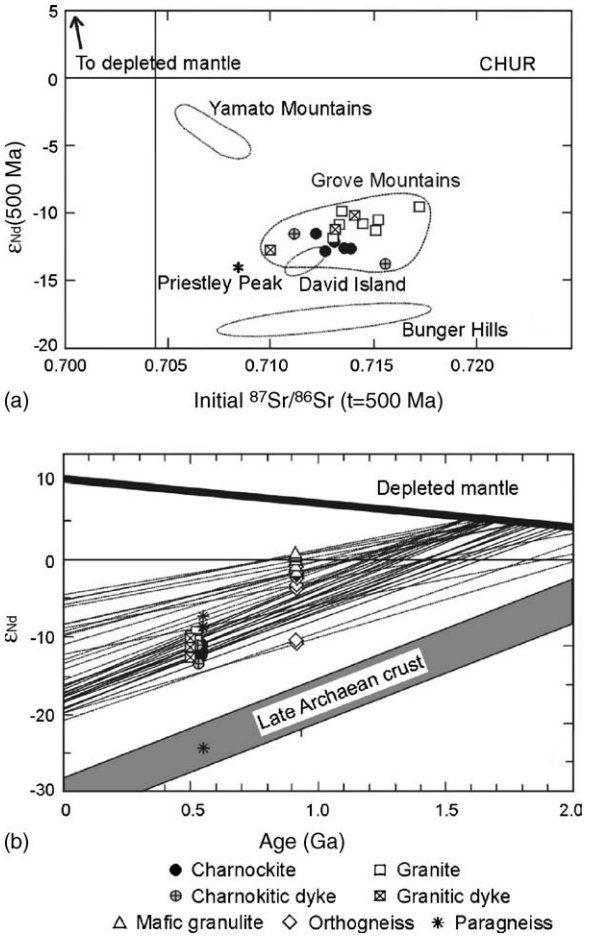

Fig. 11. (a) Plot of initial ε_{Nd} (500 Ma) vs. initial $^{87}Sr/^{86}Sr$ (t = 500 Ma) for granitoids from the Grove Mountains as well as syenitic or alkaline basaltic rocks from Priestley Peak (Nelson and McCulloch, 1989), Bunger Hills (Sheraton et al., 1990), David Island (Sheraton et al., 1992) and the Yamato Mountains (Zhao et al., 1995a). (b) Nd evolution diagram for granitoids and metamorphic rocks from the Grove Mountains.

processes of granite magma generation. The observed high Y/Nb ratios (>1.18) are also consistent with such interpretation (Eby, 1992).

As mentioned previously, there are two types of granite in the Grove Mountains. Type I granites intruded in charnockites and have low total REE contents and small negative Eu anomalies; Type II granites intruded in orthogneisses and have high total REE contents and large negative Eu anomalies. The difference in Eu anomaly between them seems to suggest a differential feldspar fractionation during magmatic evolution. However, this suggestion cannot be substantiated by the globally similar contents in Na_2O, K_2O, or A/NK and K_2O/Na_2O ratios. Trace element abundances of Rb, Sr and Ba do not support such a suggestion either. It is likely that the Eu anomaly and REE abundances are controlled by the source rocks. Taking into account the different occurrences and emplacement ages, we suggest a two-stage partial melting model. Type II granites probably experienced limited differentiation dominated by separation of feldspar, but Type I granites were generated in high-pressure partial melting of a basaltic source at deep levels.

Granitic dykes also have high I_{Sr} values, very negative $\varepsilon_{Nd}(T)$ values and Paleoproterozoic Nd model ages, completely in line with those of granites. This suggests the same source for both rocks. However, the low SiO_2 contents and relatively small negative Nb, Sr, P, Ti anomalies (see Fig. 8) demonstrate that these granitic dykes were not derived from older granites, as most dykes and pegmatites worldwide are due to the latest emplacement of residual magma from a chamber. They were probably produced by a separate, slightly high degree of partial melting of the basaltic source, and later underwent a limited fractionation of feldspar, ilmenite and apatite.

9. Tectonic setting of granitoids

Charnockite plutons are generally intruded into high-grade terranes immediately after peak granulite metamorphism (e.g. Zhao et al., 1997; Young et al., 1997). Therefore, the emplacement age of 547 ± 1 Ma obtained for the charnockite constrains the peak granulite facies metamorphism in the Grove Mountains to ca. 550 Ma. On the other hand, the last magmatic activity was marked by the emplacement of granitic dykes at 501 ± 7 Ma. As shown previously, the emplacement pressures of 5.0–6.1 kbar for granitoids are very similar to the peak metamorphic pressures of 6.1–6.7 kbar at ca. 850 °C (Liu et al., 2003b). If so, a near-isobaric cooling (IBC) from ca. 850 °C could be inferred to last for about 50 Ma for the high-grade rocks of the Grove Mountains. However, a higher pressure relic (9.3 kbar at 800 °C) preserved in a garnet-bearing granulite (Yu et al., 2002), together with the relict compressive deformation (D_1) developed in some places, undoubtedly indicates an early crustal thickening. Thus, this IBC path actually followed an earlier near-isothermal decompression (ITD) (Fig. 12) as a result of crustal extension and magmatic underplating (Harley, 1989). The development of characteristic subhorizontal structures (D_2) in such an isobarically cooled granulite terrane also reflects the extensional collapse (Sandiford, 1989). Therefore, all the petrology, structural feature and geochronology suggest that the granitoids of the Grove Mountains intruded in the extensional environment of formerly overthickened crust.

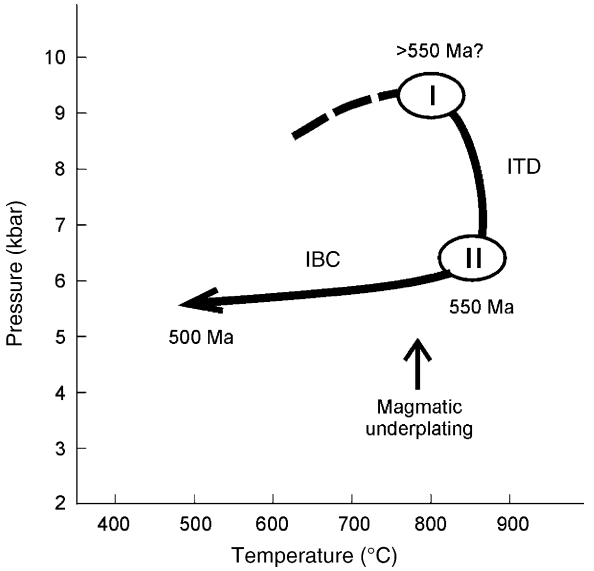

Fig. 12. The *P–T* path for the Grove Mountains. ITD and IBC represent isothermal decompression and isobaric cooling, respectively. Field I is from Yu et al. (2002) and Field II from Liu et al. (2003b).

This inference is supported by the field relations and geochemical signatures of the granitoids. Recall that charnockites with weak foliation were emplaced in metamorphic rocks during late D_2, whereas subsequent sheeted granitoids are often an indicator of deeper emplacement in an extensional environment (Nédélec et al., 1995). Geochemically, all the granitoids from the Grove Mountains share the same characteristics as A-type granites, whilst A-type granite magmatism is generally a diagnostic feature of post-collisional extensional collapse (Sylvester, 1989). In the tectonic discrimination diagram of Pearce et al. (1984), most granitoids (with exception of some granites) fall in the WPG field. As pointed out by Förster et al. (1997), late- or post-collisional granites in a continent–continent collision setting tend to produce a WPG affinity. In fact, underplating of mantle-derived mafic magma as a consequence of lithospheric delamination and asthenospheric upwelling often occurs during post-collisional extension of an orogen. Whilst the intrusion of magma produced by partial melting of underplating materials or the older lower crust rocks into the middle crust results in a near-IBC path of granulites. Thus, IBC following an ITD path of granulites, mantle-derived magma underplating, and granitic magma intrusion are interrelated, and could be indicative of continental collision zones.

Granitic dykes crosscut all the structures and hence should be of post-tectonic origin. Sr and Nd isotopic data indicate that their genesis is related to syn-orogenic charnockites and post-orogenic granites. This magmatic activity has extended to the nPCM (Manton et al., 1992; Carson et al., 2000), where no overprinting by the Pan-African high-grade metamorphism is observed. Sheraton and Black (1988) interpreted this ca. 500 Ma igneous event as the internal fracturing of Gondwana supercontinent before the eventual breakup. However, the development of locally compressional deformation in the nPCM (Boger et al., 2002) suggests that the East Antarctic Shield was not in a stable extensional regime at this time. Therefore, we propose that the occurrence of ca. 500 Ma dyke swarm marks the termination of the Pan-African tectonic evolution in Gondwana.

10. Nature and role of the Prydz Belt

Among four major Pan-African belts in the East Antarctic Shield—central Dronning Maud Land, Lützow-Holm Bay, Prydz Bay and Denman Glacier, the first two (central Dronning Maud Land and Lützow-Holm Bay), together with southern India and Sri Lanka, belong to the southern extension of the East African Orogen (Mozambique belt) based on the reconstruction of Gondwana. Because the East African Orogen has preserved a complete record from the opening of the Mozambique ocean through arc accretion to continental collision, and finally followed by extensional collapse in the ca. 900–500 Ma interval (Stern, 1994; Meert and Van der voo, 1997), most geologists have accepted central Dronning Maud Land and Lützow-Holm Bay as a portion of the final collisional zone between East and West Gondwana (e.g. Shiraishi et al., 1994; Kriegsman, 1995; Shackleton, 1996; Wilson et al., 1997; Jacobs et al., 1998, 2003). By contrast, Prydz Bay and Denman Glacier are in the interior of the hypothesized unified East Gondwana, hence the nature and role of Pan-African events in these areas is ambiguous due to the absence of subduction-related evidence (Yoshida et al., 2003 and references therein).

Despite of the absence of direct evidence for ocean closure, the compressional and extensional deformation patterns and clear decompressional textures are preserved in metamorphic rocks from Prydz Bay (Dirks and Wilson, 1995; Carson et al., 1995, 1997; Fitzsimons, 1996). This is compatible with a collisional orogeny followed by extensional collapse of a thickened crust. The Grove Mountains slightly differ from Prydz Bay in containing voluminous syn- to post-orogenic charnockites and sheeted granites. The emplacement of such granitoids into middle crust results in a near-IBC path following ITD for the granulite terrane and a slow exhumation of reheated crust. Importantly, this type of *P–T* evolution has also been documented in

the late Pan-African granulites from the East African Orogen (e.g. Kröner et al., 2001). In comparison, the Grove Mountains closely resemble central Dronning Maud Land by the effect of late Pan-African high-grade metamorphism (Jacobs et al., 2003), a near-IBC path following ITD (Ravikant, 1998) and syn- to post-orogenic magmatic evolution (Paulsson and Austrheim, 2003). It seems that the Prydz Belt has preserved the record of a collisional event analogous to the late evolutionary stage of the East African Orogen. Therefore, the petrological, geochronological and geochemical data in this study support the inference that the Prydz Belt represents an orogen formed by collision between the Indo-Antarctic and Australo-Antarctic continental blocks.

As Harley (2003) discussed, each of the Archaean cratonic blocks within the East Antarctic Shield recorded distinct evolutionary histories and did not form a single unified craton. Moreover, Fitzsimons (2000a,b) demonstrated that there were two distinct Grenvillian provinces on the two sides of the Prydz Belt, i.e. the Rayner province (including nPCM and Mawson Coast) of 990–900 Ma and the Wilkes province (including Windmill Islands and Bunger Hills) of 1330–1130 Ma. Hence, he argued that no single continuous Grenvillian mobile belt around the East Antarctic coastline had ever been formed. Paleomagnetic data showed that the apparent polar wander path for the India and Australo-Antarctic continental blocks did not form a spatially and temporally coherent pattern until ca. 550 Ma (Meert and Van der voo, 1997; Powell and Pisarevsky, 2001). All these data strongly suggest that East Gondwana was not assembled until late Pan-African time.

However, the absence of diagnostic rocks for a suture, such as an ophiolite suite, accretionary complex and high-pressure metamorphic rock, has weakened the argument of this issue, even though it could be argued that these indicator rocks were completely removed in the deeply eroded orogens (Key et al., 1989; Kröner and Cordani, 2003). The Grenvillian precursors have been proved to occur in the Pan-African Prydz Belt (Zhao et al., 1993; Hensen and Zhou, 1995), but it is still not clear what has happened in the ca. 1000–550 Ma interval. Based on the limited geochronological data from Prydz Bay, some authors (Hensen and Zhou, 1995; Zhao et al., 1995b; Fitzsimons, 1997) suggest a young, Neoproterozoic sedimentation from the Paleoproterozoic sources on the Grenvillian basements, and Zhao et al. (2003) therefore promote an accretionary model to explain the evolution of the Prydz Belt. The new SHRIMP U–Pb zircon dating reveals that a Neoproterozoic igneous event of 910–920 Ma was preserved in mafic granulites and orthogneisses from the Grove Mountains (our unpublished data). This event may be related to the end of the Grenvillian orogeny or may signify the beginning of the break-up of Rodinia (Kröner et al., 2003). Obviously, further investigation on the Neoproterozoic crustal history of the Prydz Belt is necessary and it may hold the key to understanding the tectonic process between Indo-Antarctic and Australo-Antarctic continental blocks.

11. Conclusions

(1) The high-grade metamorphic complex and intrusives from the Grove Mountains, East Antarctica, are an inland continuation of the Pan-African Prydz Belt. The diverse granitoids—charnockite, charnockitic dykes, granite and granitic dykes are dated at 547 ± 1, 533 ± 3, 503 ± 2 and 501 ± 7 Ma, respectively. The new age data suggest a prolonged magmatic activity lasting for ca. 50 Ma from syn- to post-orogeny.

(2) Based on geochemistry and Sr–Nd isotopic characteristics, the generation of the granitoids has involved a similar source (enriched alkaline basalt) but different processes during partial melting. High-temperature partial melting of the basaltic source produced charnockites and fractionated charnockitic dykes, whereas granites and granitic dykes were formed by partial melting of such a source accompanied by crustal contamination.

(3) The Grove Mountains have experienced an earlier higher pressure granulite facies metamorphism during crustal thickening, followed by high-temperature metamorphism during crustal extension. The underplating of mantle-derived magma and emplacement of granitoids resulted in a near-isothermal decompression followed by near-isobaric cooling of the terrane. This *P–T* path is indicative of a continental collision zone.

(4) The whole Prydz Belt has preserved the entire record of an orogenic process including crustal thickening, extensional collapse and syn- to post-orogenic magmatic intrusion, which is very similar to the late stage of the East African Orogeny. Although no ophiolite suite and accretionary complex are recognized, the available data support that this belt represents a suture between the Indo-Antarctic and Australo-Antarctic continental blocks.

Acknowledgements

We would like to thank J. Li and D. Huo for assistance during field work and F.-Y. Wu and X.-H. Li for discussions. Critical reviews by N.C.N. Stephen-

son and an anonymous reviewer substantially improved the manuscript. The field work was carried out during the 1998–1999 Chinese National Antarctic Research Expedition. Logistic support by the Antarctic Administration of China and financial support by the National Natural Science Foundation of China (Nos. 40372046, 40072028), Geological Investigation Project of China Geological Survey (1212010511505), National Basic Research Project of China (2002DEA30027-8) and A Hundred Geologists Project of MLR are gratefully acknowledged. The senior author was further supported by the National Science Council (NSC) of Taiwan for the final preparation of the manuscript. Bor-ming Jahn acknowledges the financial support of NSC through grants NSC92-2811-M-002-056 and NSC-93-2116-M-002-006.

References

Anderson, J.L., Bender, E.E., 1989. Nature and origin of Proterozoic A-type granitic magmatism in the southwestern United States of America. Lithos 23, 19–52.

Black, L.P., Sheraton, J.W., Tingey, R.J., McCulloch, M.T., 1992. New U–Pb zircon ages from the Denman Glacier area, East Antarctica, and their significance for Gondwana reconstruction. Antarct. Sci. 4, 447–460.

Boger, S.D., Carson, C.J., Wilson, C.J.L., Fanning, C.M., 2000. Neoproterozoic deformation in the northern Prince Charles Mountains, East Antarctica: evidence for a single protracted orogenic event. Precambrian Res. 104, 1–24.

Boger, S.D., Carson, C.J., Wilson, C.J.L., Fanning, C.M., 2001. Early Paleozoic tectonism within the East Antarctic craton: the final suture between east and west Gondwana? Geology 29, 463–466.

Boger, S.D., Carson, C.J., Fanning, C.M., Hergt, J.M., Wilson, C.J.L., Woodhead, J.D., 2002. Pan-African intraplate deformation in the northern Prince Charles Mountains, East Antarctica. Earth Planet. Sci. Lett. 195, 195–210.

Boger, S.D., Miller, J.M., 2004. Terminal suturing of Gondwana and the onset of the Ross-Delamerian Orogeny: the cause and effect of an Early Cambrian reconfiguration of plate motions. Earth Planet. Sci. Lett. 219, 35–48.

Carson, C.J., Dirks, P.G.H.M., Hand, M., Sims, J.P., Wilson, C.J.L., 1995. Compressional and extensional tectonics in low-medium pressure granulites from the Larsemann Hills, East Antarctica. Geol. Mag. 132, 151–170.

Carson, C.J., Fanning, C.M., Wilson, C.J.L., 1996. Timing of the Progress Granite, Larsemann Hills: evidence for Early Palaeozoic orogenesis within the East Antarctica Shield and implications for Gondwana assembly. Aust. J. Earth Sci. 43, 539–553.

Carson, C.J., Powell, P., Wilson, C.J.L., Dirks, P.H.G.M., 1997. Partial melting during tectonic exhumation of a granulite terrane: an example from the Larsemann Hills, East Antarctica. J. Metamorph. Geol. 15, 105–126.

Carson, C.J., Boger, S.D., Fanning, C.M., Wilson, C.J.L., Thost, D.E., 2000. SHRIMP U–Pb geochronology from Mount Kirkby, northern Prince Charles Mountains, East Antarctica. Antarct. Sci. 12, 429–442.

Chen, B., Jahn, B.-m., Zhai, M., 2003. Sr–Nd isotopic characteristics of the Mesozoic magmatism in the Taihang-Yanshan orogen, North China craton, and implications for Archaean lithosphere thinning. J. Geol. Soc. Lond. 160, 963–970.

Choudhary, A.K., Harris, N.B.W., Van Calsteren, P., Hawkesworth, C.J., 1992. Pan-African charnockite formation in Kerala, southern India. Geol. Mag. 129, 257–264.

Dale, J., Holland, T., Powell, R., 2000. Hornblende-garnet-plagioclase thermobarometry: a natural assemblage calibration of the thermodynamics of hornblende. Contrib. Mineral. Petrol. 140, 353–362.

Dirks, P.H.G.M., Wilson, C.J.L., 1995. Crustal evolution of the East Antarctic mobile belt in Prydz Bay: continental collision at 500 Ma? Precambrian Res. 75, 189–207.

Droop, G.T.R., 1987. A general equation for estimating Fe^{3+} concentrations in ferromagnesian silicates and oxides from microprobe analyses, using stoichiometric criteria. Mineral. Mag. 51, 431–435.

Eby, G.N., 1992. Chemical subdivision of the A-type granitoids: petrogenesis and tectonic implications. Geology 20, 641–644.

Fitzsimons, I.C.W., 1996. Metapelitic migmatites from Brattstrand Bluffs, East Antarctica-metamorphism, melting and exhumation of the mid crust. J. Petrol. 37, 395–414.

Fitzsimons, I.C.W., 1997. The Brattstrand Paragneiss and the Søstrene Orthogneiss: a review of Pan-African metamorphism and Grenvillian relics in southern Prydz Bay. In: Ricci, C.A. (Ed.), The Antarctic Region: Geological Evolution and Processes. Terra Antart. Publ., Siena, pp. 121–130.

Fitzsimons, I.C.W., 2000a. A review of tectonic events in the East Antarctic Shield and their implications for Gondwana and earlier supercontinents. J. Afr. Earth Sci. 31, 3–23.

Fitzsimons, I.C.W., 2000b. Grenville-age basement provinces in East Antarctica: evidence for three separate collisional orogens. Geology 28, 879–882.

Fitzsimons, I.C.W., 2003. Proterozoic basement provinces of southern and southwestern Australia, and their correlation with Antarctica. In: Yoshida, M., Windley, B., Dasgupta, S. (Eds.), Proterozoic East Gondwana: Supercontinent Assembly and Breakup. Geol. Soc. London, Spec. Publ. 206, pp. 93–130.

Fitzsimons, I.C.W., Harley, S.L., 1991. Geological relationships in high-grade gneisses of the Brattstrand Bluffs coastline, Prydz Bay, East Antarctica. Aust. J. Earth Sci. 38, 497–519.

Fitzsimons, I.C.W., Kinny, P.D., Harley, S.L., 1997. Two stages of zircon and monazite growth in anatectic leucogneiss: SHRIMP constraints on the duration and intensity of Pan-African metamorphism in Prydz Bay, East Antarctica. Terra Nova 9, 47–51.

Förster, H.-J., Tischendorf, G., Trumbull, R.B., 1997. An evaluation of the Rb vs. (Y + Nb) discrimination diagram to infer tectonic setting of silicic igneous rocks. Lithos 40, 261–293.

Green, D.H., Lambert, I.B., 1965. Experimental crystallization of anhydrous granite at high pressures and temperatures. J. Geophys. Res. 70, 5259–5268.

Green, T.H., Watson, E.B., 1982. Crystallization of apatite in natural magmas under high pressure, hydrous conditions, with particular reference to 'orogenic' rock series. Contrib. Mineral. Petrol. 79, 96–105.

Green, T.J., Pearson, N.J., 1986. Ti-rich accessory phase saturation in hydrous mafic-felsic compositions at high P, T. Chem. Geol. 54, 185–201.

Goscombe, B., Armstrong, R., Barton, J.M., 1998. Tectonometamorphic evolution of the Chewore inliers: partial re-equilibration of high-grade basement during the Pan-African orogeny. J. Petrol. 39, 1347–1384.

Halliday, A.N., Davidson, J.P., Hilderth, W., Holden, P., 1991. Modelling the petrogenesis of high Rb/Sr silicic magmas. Chem. Geol. 92, 107–114.

Harley, S.L., 1989. The origins of granulites: a metamorphic perspective. Geol. Mag. 126, 215–247.

Harley, S.L., 2003. Archaean-Cambrian crustal development of East Antarctica: metamorphic characteristics and tectonic implications. In: Yoshida, M., Windley, B., Dasgupta, S. (Eds.), Proterozoic East Gondwana: Supercontinent Assembly and Breakup. Geol. Soc. London, Spec. Publ. 206, pp. 203–230.

Harley, S.L., Snape, I., Black, L.P., 1998. The early evolution of a layered metaigneous complex in the Rauer Group, East Antarctica: evidence for a distinct Archaean terrane. Precambrian Res. 89, 175–205.

Hensen, B.J., Zhou, B., 1995. A Pan-African granulite facies metamorphic episode in Prydz Bay, Antarctica: evidence from Sm–Nd garnet dating. Aust. J. Earth Sci. 42, 249–258.

Hensen, B.J., Zhou, B., 1997. East Gondwana amalgamation by Pan-African collision? Evidence from Prydz Bay, East Antarctica. In: Ricci, C.A. (Ed.), The Antarctic Region: Geological Evolution and Processes. Terra Antart. Publ., Siena, pp. 115–119.

Holland, T., Blundy, J., 1994. Non-deal interactions in calcic amphiboles and their bearing on amphibole–plagioclase thermometry. Contrib. Mineral. Petrol. 116, 433–447.

Jacobs, J., Fanning, C.M., Henjes-Kunst, F., Olesch, M., Paech, H.-J., 1998. Continuation of the Mozambique Belt into East Antarctica: Grenville-age metamorphism and polyphase Pan-African high-grade events in central Dronning Maud Land. J. Geol. 106, 385–406.

Jacobs, J., Bauer, W., Fanning, C.M., 2003. Late Neoproterozoic/Early Palaeozoic events in central Dronning Maud Land and significance for the southern extension of the East African Orogen into East Antarctica. Precambrian Res. 126, 27–53.

John, B.E., Blundy, J.D., 1994. Emplacement-related deformation of granitoid magmas, southern Adamello Massif, Italy. Geol. Soc. Am. Bull. 105, 155–164.

Kelsey, D.E., Powell, R., Wilson, C.J.L., Steele, D.A., 2003. (Th + U)–Pb monazite ages from Al–Mg-rich metapelites, Rauer Group, East Antarctica. Contrib. Mineral. Petrol. 146, 326–340.

Keto, L.S., Jacobsen, S.B., 1987. Nd and Sr isotopic variations of Early Paleozoic oceans. Earth Planet. Sci. Lett. 84, 27–41.

Key, R.M., Charsley, T.J., Hackman, B.D., Wilkinson, A.F., Rundle, C.C., 1989. Superimposed upper Proterozoic collision-controlled orogenies in the Mozambique orogenic belt of Kenya. Precambrian Res. 44, 197–212.

Kilpatrick, J.A., Ellis, D.J., 1992. C-type magmas: igneous charnockites and their extrusive equivalents. Trans. R. Soc. Edinb.: Earth Sci. 83, 155–164.

Kriegsman, L.M., 1995. The Pan-African event in East Antarctica: a view from Sri Lanka and the Mozambique Belt. Precambrian Res. 75, 263–277.

Krogh, T.E., 1973. A low-contamination method for hydrothermal decomposition of zircon and extractions of U and Pb for isotopic age determinations. Geochim. Cosmochim. Acta 37, 485–494.

Krogh, T.E., 1982. Improved accuracy of U–Pb zircon dating by the creation of more concordant systems using air abrasion technique. Geochim. Cosmochim. Acta 46, 637–649.

Kröner, A., Williams, I.S., 1993. Age of metamorphism in the high-grade rocks of Sri Lanka. J. Geol. 101, 513–521.

Kröner, A., Willner, A.P., Hegner, E., Jaeckel, P., Nemchin, A., 2001. Single zircon ages, PT evolution and Nd isotopic systematics of high-grade gneisses in southern Malawi and their bearing on the evolution of the Mozambique belt in southeastern African. Precambrian Res. 109, 257–291.

Kröner, A., Cordani, U., 2003. African, southern Indian and South American cratons were not part of the Rodinia supercontinent: evidence from field relationships and geochronology. Tectonophysics 375, 325–352.

Kröner, A., Kehelpannala, K.V.W., Hegner, E., 2003. Ca. 750–1100 Ma magmatic events and Grenville-age deformation in Sri Lanka: relevance for Rodinia supercontinent formation and dispersal, and Gondwana amalgamation. J. Asian Earth Sci. 22, 279–300.

Liu, X.C., Zhao, Y., Liu, X.H., 2002. Geological aspects of the Grove Mountains, East Antarctica. In: Gamble, J.A., Skinner, D.N.B., Henrys, S. (Eds.), Antarctica at the Close of a Millennium. R. Soc. New Zealand Bull. 35, pp. 161–166.

Liu, X.H., Zhao, Y., Liu, X.C., Yu, L., 2003a. Geology of the Grove Mountains in East Antarctica—new evidence for the final suture of Gondwana Land. Sci. China (Ser. D) 46, 305–319.

Liu, X.C., Zhao, Z., Zhao, Y., Chen, J., Liu, X.H., 2003b. Pyroxene exsolution in mafic granulites from the Grove Mountains, East Antarctica: constraints on the Pan-African metamorphic conditions. Eur. J. Mineral. 15, 55–65.

Maniar, P.D., Piccoli, P.M., 1989. Tectonic discrimination of granitoids. Geol. Soc. Am. Bull. 101, 635–643.

Manton, W.I., Grew, E.S., Ghofmann, J., Sheraton, J.W., 1992. Granitic rocks of the Jetty Peninsula, Amery Ice Shelf area, East Antarctica. In: Yoshida, Y., Kaminuma, K., Shiraishi, K. (Eds.), Recent Progress in Antarctic Earth Science. Terra Scientific Publishing Company, Tokyo, pp. 179–189.

McCulloch, M.T., Gamble, J.A., 1991. Geochemical and geodynamical constraints on subduction zone magmatism. Earth Planet. Sci. Lett. 102, 358–374.

Meert, J.G., 2003. A synopsis of events related to assembly of eastern Gondwana. Tectonophysics 362, 1–40.

Meert, J.G., Van der voo, R., 1997. The assembly of Gondwana 800–550 Ma. J. Geodynam. 23, 223–235.

Mikhalsky, E.V., Sheraton, J.W., Beliatsky, B.V., 2001. Preliminary U–Pb dating of Grove Mountains rocks: implications for the Proterozoic to Early Palaeozoic tectonic evolution of the Lambert Glacier-Prydz Bay area (East Antarctica). Terra Antarct. 8, 3–10.

Naney, M.T., 1983. Phase equilibria of rock-forming silicates in granitic systems. Am. J. Sci. 283, 993–1033.

Nédélec, A., Stephens, W.E., Fallick, N.E., 1995. The Panafrican stratoid granites of Madagascar: alkaline magmatism in a post-collisional extensional setting. J. Petrol. 36, 1367–1391.

Nelson, D.R., McCulloch, M.T., 1989. Enriched mantle components and mantle recycling of sediments. In: Ross, J. (Ed.), Kimberlites and Related Rocks: Their Composition, Occurrence, Origin and Emplacement, vol. 1. Geol. Soc. Aust., Spec. Publ. 14, pp. 560–570.

Paquette, J.L., Nédélec, A., Moine, B., Rakotondrazafy, M., 1994. U–Pb, single zircon Pb-evaporation, and Sm–Nd isotopic study of a granulite domain in SE Madagascar. J. Petrol. 102, 523–538.

Paulsson, O., Austrheim, H., 2003. A geochronological and geochemical study of rocks from Gjesvikfjella, Dronning Maud Land, Antarctica—implications for Mesoproterozoic correlations and assembly of Gondwana. Precambrian Res. 125, 113–138.

Pearce, J.A., Harris, N.B.W., Tindle, A.G., 1984. Trace element discrimination diagrams for the interpretation of granitic rocks. J. Petrol. 25, 956–983.

Powell, C.McA., Pisarevsky, S.A., 2001. Late Neoproterozoic assembly of East Gondwana. Geology 30, 3–6.

Ravikant, V., 1998. Preliminary thermal modeling of the massif anorthosite-charnockitic gneiss interface from Gruber Mountains, central Dronning Maud Land, East Antarctica. J. Geol. Soc. India 52, 287–300.

Sandiford, M., 1989. Horizontal structures in granulite terrains: a record of mountain building or mountain collapse? Geology 17, 449–452.

Schmidt, M.W., 1992. Amphibole composition in tonalite as a function of pressure: an experimental calibration of the Al-in-hornblende barometer. Contrib. Mineral. Petrol. 110, 304–310.

Shackleton, R.M., 1996. The final collision zone between East and West Gondwana: where is it? J. Afr. Earth Sci. 23, 271–287.

Sheraton, J.W., Black, L.P., 1988. Chemical evolution of granitic rocks in the East Antarctic Shield, with particular reference to post-orogenic granites. Lithos 21, 37–52.

Sheraton, J.W., Black, L.P., McCulloch, M.T., Oliver, R.L., 1990. Age and origin of a compositionally varied mafic dyke swarm in the Bunger Hills, East Antarctica. Chem. Geol. 85, 215–246.

Sheraton, J.W., Black, L.P., Tindle, A.G., 1992. Petrogenesis of plutonic rocks in a Proterozoic granulite-facies terrane—the Bunger Hills, East Antarctica. Chem. Geol. 97, 163–198.

Sheraton, J.W., Tindle, A.G., Tingey, R.J., 1996. Geochemistry, origin, and tectonic setting of granitic rocks of the Prince Charles Mountains, Antarctica. AGSO J. Aust. Geol. Geophys. 16, 345–370.

Shiraishi, K., Hiroi, Y., Ellis, D.J., Fanning, C.M., Motoyoshi, Y., Nakai, Y., 1992. The first report of a Cambrian orogenic belt in East Antarctica—an ion microprobe study of the Lützow-Holm Complex. In: Yoshida, Y., Kaminuma, K., Shiraishi, K. (Eds.), Recent Progress in Antarctic Earth Science. Terra Scientific Publishing Company, Tokyo, pp. 29–35.

Shiraishi, K., Ellis, D.J., Hiroi, Y., Fanning, C.M., Motoyoshi, Y., Nakai, Y., 1994. Cambrian orogenic belt in East Antarctica and Sri Lanka: implications for Gondwana assembly. J. Geol. 102, 47–65.

Stern, R.J., 1994. Arc assembly and continental collision in the Neoproterozoic East African Orogen: implications for the consolidation of Gondwanaland. Ann. Rev. Earth Planet. Sci. 22, 319–351.

Streckeisen, A., Le Maitre, R.W., 1979. A chemical approximation to the modal QAPF classification of the igneous rocks. Neues Jahrb. Mineral., Abh. 136, 169–206.

Stüwe, K., Powell, R., 1989. Low pressure granulite facies metamorphism in the Larsemann Hills area, East Antarctica: Petrology and tectonic implications for the Prydz Bay area. J. Metamorph. Geol. 7, 465–484.

Sun, S.S., McDonough, W.E., 1989. Chemical and isotopic systematics of oceanic basalts: implications for mantle composition and processes. In: Saunders, A.D., Norry, M.J. (Eds.), Magmatism in the Ocean Basins. Geol. Soc., Spec. Publ, pp. 313–345.

Sylvester, P.J., 1989. Post-collisional alkaline granites. J. Geol. 97, 261–280.

Taylor, S.R., McLennant, S.M., 1985. The Continental Crust: Its Composition and Evolution. Blackwell, Oxford, 312 pp.

Thost, D.E., Hensen, B.J., Motoyoshi, Y., 1994. The geology of a rapidly uplifted medium and low pressure granulite facies terrane of Pan African age: the Bolingen Islands, Prydz Bay, East Antarctica. Petrology 2, 293–316.

Wang, L., He, H., Li, B., 2003. Multi-element determination in geological samples by inductively coupled plasma mass spectrometry after fusion-precipitation treatment. Rock Mineral Anal. 22, 86–92 (in Chinese with English abstract).

Whalen, J.B., Currie, K.L., Chappell, B.W., 1987. A-type granites: geochemical characteristics, discrimination and petrogenesis. Contrib. Mineral. Petrol. 95, 407–419.

Wilson, T.J., Grunow, A.M., Hanson, R.E., 1997. Gondwana assembly: the view from southern Africa and East Gondwana. J. Geodynam. 23, 263–286.

Wu, F.-Y., Sun, D.-Y., Li, H.-M., Jahn, B.-m., Wilde, S., 2002. A-type granites in northeastern China: age and geochemical constraints on their petrogenesis. Chem. Geol. 187, 143–173.

Xie, Z., Chen, J.-F., Zheng, Y.-F., Zhang, X., Li, H.-M., Zhou, T.-X., 2001. Zircon U–Pb dating of the metamorphic rocks of different grades from the southern part of the Dabie terrain in China. Phys. Chem. Earth A 26, 685–693.

Yang, J.-H., Chung, S.-L., Zhai, M.-G., Zhou, X.-H., 2004. Geochemical and Sr–Nd–Pb isotopic compositions of mafic dikes from the Jiaodong Peninsula, China: evidence for vein-plus-peridotite melting in the lithospheric mantle. Lithos 73, 145–160.

Yoshida, M., 1995. Cambrian orogenic belt in East Antarctica and Sri Lanka: implications for Gondwana assembly: a discussion. J. Geol. 103, 467–468.

Yoshida, M., Jacobs, J., Santosh, M., Rajesh, H.M., 2003. Role of Pan-African events in the Circum-East Antarctic Orogen of East Gondwana: a critical overview. In: Yoshida, M., Windley, B., Dasgupta, S. (Eds.), Proterozoic East Gondwana: Supercontinent Assembly and Breakup. Geol. Soc. London, Spec. Publ. 206, pp. 57–75.

Young, D.N., Zhao, J.-x., Ellis, D.J., McCulloch, M.T., 1997. Geochemical and Sr–Nd isotopic mapping of source provinces for the Mawson charnockites, East Antarctica: implications for Proterozoic tectonics and Gondwana reconstruction. Precambrian Res. 86, 1–19.

Yu, L., Liu, X.H., Zhao, Y., Ju, Y., Liu, X.C., 2002. Metamorphism of mafic granulites in the Grove Mountains, East Antarctica. Acta Petrol. Sin. 18, 501–516 (in Chinese with English abstract).

Zhao, Y., Song, B., Wang, Y., Ren, L., Li, J., Chen, T., 1992. Geochronology of the late granite in the Larsemann Hills, East Antarctica. In: Yoshida, Y., Kaminuma, K., Shiraishi, K. (Eds.), Recent Progress in Antarctic Earth Science. Terra Scientific Publishing Company, Tokyo, pp. 155–161.

Zhao, Y., Song, B., Zhang, Z., Fu, Y., Chen, T., Wang, Y., Ren, L., Yao, Y., Li, J., Liu, X.H., 1993. An Early Palaeozoic ('Pan African') thermal event in the Larsemann Hills and its neighbours, Prydz Bay, East Antarctica. Sci. China (Ser. B) 23, 1001–1008 (in Chinese).

Zhao, J.-X., Shiraishi, K., Ellis, D.J., Sheraton, J.W., 1995a. Geochemical and isotopic studies of syenites from the Yamato Mountains, East Antarctica: implications for the origin of syenitic magmas. Geochim. Cosmochim. Acta 59, 1363–1382.

Zhao, Y., Liu, X.H., Song, B., Zhang, Z., Li, J., Yao, Y., Wang, Y., 1995b. Constraints on the stratigraphic age of metasedimentary rocks from the Larsemann Hills, East Antarctica: possible implications for Neoproterozoic tectonics. Precambrian Res. 75, 175–188.

Zhao, J.-X., Ellis, D.E., Kilpatrick, J.A., McCulloch, M.T., 1997. Geochemical and Sr–Nd isotopic study of charnockites and related rocks in the northern Prince Charles Mountains, East Antarctica: implications for charnockite petrogenesis and Proterozoic crustal evolution. Precambrian Res. 81, 37–66.

Zhao, Y., Liu, X.C., Fanning, C.M., Liu, X.H., 2000. The Grove Mountains, a segment of a Pan-African orogenic belt in East Antarctica. Abstract Volume of the 31th IGC, Rio de Janeiro, Brazil.

Zhao, Y., Liu, X.H., Liu, X.C., Song, B., 2003. Pan-African events in Prydz Bay, East Antarctica and its inference on East Gondwana tectonics. In: Yoshida, M., Windley, B., Dasgupta, S. (Eds.), Proterozoic East Gondwana: Supercontinent Assembly and Breakup. Geol. Soc. London, Spec. Publ. 206, pp. 231–245.